The Sextupole Scheme for the Swiss Light Source (SLS): An Analytic Approach

SLS Note 9/97

Johan Bengtsson

Paul Scherrer Institut (PSI)
Villigen, Switzerland

March 7, 1997

Abstract

We have applied modern techniques for single particle Hamiltonian dynamics to be able to pursue self-consistent modeling for both numerical evaluation and analytical studies. These techniques made it feasible to pursue a systematic approach in the design towards a sextupole scheme for the Swiss Light Source (SLS). The derivation of analytical formula to obtain insight into the parameter dependence of various dynamical properties was simplified considerable by the use of map normal form rather than traditional Hamiltonian perturbation theory. In the process we also verified that perturbation theory works fairly well for regions of phase space where the motion is regular, hence allowing us to model and reduce the effecs of the nonlinear perturbations.

Contents

1 Introduction

We would like to start by informing the reader that a critical point of view will be taken in the following presentation. In particular when contrasting here applied state of the art techniques against more old-fashioned. The main reason originates from the observation that the scientific process is not always as rational it likes to presume. We also prefer to view the many models appearing in this field, including our owns, as little more than temporary approximations, eventually to be replaced when more sophisticated methods appears on the horizon. Furthermore, often heard claims like: "Existing accelerator works." or "Everything in the control room is linear." have of course little scientific content due to their inherent lack of precision.

In any case, a critical presentation can only aid to clarify matters for the skeptical yet open-minded reader that prefers to draw his own conclusions based on his own judgment. In particular, any newcomer to a field that has to confront such a broad range of physical phenomena. And yet, often unnecessarily obscured by an individual tendency to overemphasize differences in techniques rather than first establishing the common ground, rarely beyond classical electrodynamics, from which the various advantages of the different techniques would emerge in broad daylight. We therefore partly sympathize with the slow acceptance among the many potential users that could benefit from these new methods. See ref. [1] for an excellent general scientific review, ref. [2][1] for the more typical subjective, and ref. [3] for an attempt to reach a coherent presentation from the experts.

In fact, we challenge the mathematically inclined reader to try to extract a coherent picture[2] from the presentations in these publications noting that they are, apart from the quantum fluctuations in synchrotron radiation, applications of classical electrodynamics [4]. On time scales where the effect of synchrotron radiation can be ignored, the guiding principles for the various techniques presented in these papers may be summarized as: relativistic single particle Hamiltonian dynamics [5] taking advantage of the underlying

[1]The following references may serve as a set of papers complementing each other for the reader interested in acquiring a somewhat broader point of view: basic Lie algebraic techniques for accelerators [60, 61, 62, 63, 64, 65], generating function techniques [66, 67, 68], symplectic integrators [69, 70, 71, 72, 73, 74, 75, 76, 77], truncated Power Series Algebra (TPSA) [78, 79, 80, 81, 82], map normal form [83, 84, 85, 86], synchrotron radiation [87, 88, 89, 90, 92], accelerator modeling and design [91, 92, 93, 94, 95, 96, 97, 98].

[2]Ref. [1, 90] are two exceptions that may be viewed as a "proof of principle".

Lie algebraic structure of Hamilton's equations to numerically integrate or, by using Truncated Power Series Algebra (TPSA) [6] for Automatic Differentiation (AD) [7], evaluate, concatenate, extract and bring perturbatively into normal form [8, 9] the corresponding symplectic maps.

We emphasize that even though the presented work was carried out for the Swiss Light Source (SLS), the applied methodology is completely general and suitable for any synchrotron. We will in the following therefore view SLS as an example. Like any modern high performance synchrotron, it has a magnetic lattice with very strong focusing and large natural chromaticity which as usual is compensated by chromatic sextupoles. Since these then also are relatively strong, the stability is governed by the corresponding nonlinear dynamics.[3]

We are from a general point of view dealing with a confinement problem. The study is complicated by the fact that different dynamical processes are important on different time scales. They may be classified roughly as:

- First-turn: injection, first turn (single-pass) and closed orbit.
- Short-term: a few synchrotron oscillations, typically 10^2 turns; betatron- and synchro-betatron motion and related resonances.
- Medium-term: one damping time, typically 10^4 turns; synchrotron radiation (classical radiation, quantum fluctuations determining the equilibrium emittance), and wake-field effects.
- Long-term: typically 10^9 turns; residual gas scattering, Touschek scattering, and beam-beam interaction.

These are traditionally addressed by a step-wise process where one first establishes a lattice with reasonable short term stability. The other time scales can then be analyzed, often by models parameterized in terms of global properties of the short-term dynamics [16, 17, 18, 19]. Refined considerations for

[3]SLS is a third generation synchrotron light source with state of the art brightness primarily obtained by pushing the emittance. The linear optics design for such a source, is a nontrivial nonlinear optimization problem which will not be addressed here. This can to some degree be appreciated by the elementary fact that even though in itself a linear stability problem, a realistic lattice design requires careful tailoring of related lattice functions with strong nonlinear dependence on the magnet strengths. For these aspects see [10, 11, 12, 13, 14]. The finally adopted lattice, based on a triple-bend-achromat structure [15] was developed by A. Streun [13, 14]

the injection process or estimated life times may lead to new requirements on some of the global properties and the lattice design becomes an iterative process.

A fundamental problem for a systematic search of a solution for the confinement problem, is the lack of a complete theory for stability in the nonlinear case. The elegance and simplicity of linear control theory originates from the fact that stability, controllability- and observability of a system can be determined directly from certain algebraic properties of the mathematical model. In particular, the eigenvalues of the state matrix[4] and the rank of the controllability and observability matrix.[5] For the nonlinear case, stability depends in general also on the initial conditions, and one is forced to study the stability of individual trajectories for given initial conditions by numerical integration, so called *tracking*.

Application of sophisticated mathematical methods has led to the well known KAM-theorem [22], stating roughly that a system with periodic solutions has quasi-periodic solutions for sufficiently small perturbations. But this theorem is unfortunately rather academic, i.e. solution exists..., and has found little use in quantitative accelerator design, the crux originating from the definition of a sufficiently small perturbation.[6] We therefore have to rely on a more intuitive approach, arguing that the long term stability ought be improved by reducing the leading order nonlinear perturbations, since this brings the equations of motion closer to the linear approximation for which linear stability has been established in the process of linear lattice design. The argument can be made somewhat sharper by considering the parametric variation of the tune with for example the momentum deviation δ. If one considers an ensemble of particles over δ, one may expect stability problems for particles with an actual tune close to any betatron resonance driven by the magnetic lattice. For electrons, one may of course argue that stability over one damping time should be sufficient for stability over all times. But this is naive since the electrons will in general be slowly crossing resonances

[4] First applied to the alternating gradient synchrotron by Courant and Snyder [20] by analyzing the state matrix (the one-turn transport matrix).

[5] See any textbook on the subject or [21] for a straightforward application to Hill's equation.

[6] To quote I. Percival [23]: "In fact Hénon showed Arnold's proof only applies if the perturbation is less than 10^{-333} and Moser's if it is less than 10^{-48}, in appropriate units. The latter is less than the gravitation perturbation of a football in Spain by the motion of a bacterium in Australia!"

in their trajectories of damped betatron oscillations towards the equilibrium orbit. In particular just after injection and a Touschek event.

Systematic accelerator design relies on the fact that modern techniques allows one to easily and self-consistently[7] test such a hypothesis against numerical simulations based on precise models that describes the single particle dynamics on the short- and medium-term time scales. Effectively, the accelerator physicist's economy version of the aerodynamicist's "wind tunnel". At large, feasible of course due to the relative simplicity of dynamics for systems described by ordinary- rather than partial differential equations.

2 The Equations of Motion

The effect of synchrotron radiation can be neglected in the following treatment since we are primarily concerned about control of the short term dynamics. This approximation is pursued for simplicity, since classical radiation can be accommodated in the underlying theoretical framework by generalizing from a Hamiltonian flow to a vector field whenever required [3].

2.1 The Relativistic Hamiltonian

The Hamiltonian for a charged particle in an external electromagnetic field transformed into the local comoving frame customarily used for accelerators is given by [5, 20]

$$\begin{aligned} H_1\left(x, p_x, y, p_y, -p_t, ct; s\right) = & -\left[1 + h_{ref}\left(s\right) x\right] \\ & \times \left\{ \frac{q}{p_0} A_s\left(s\right) + \sqrt{1 - \frac{2}{\beta} p_t + p_t^2 - \left[p_x - \frac{q}{p_0} A_x\left(s\right)\right]^2 - \left[p_y - \frac{q}{p_0} A_y\left(s\right)\right]^2} \right\} \end{aligned} \tag{1}$$

where

$$p_t \equiv -\frac{E - E_0}{p_0 c}, \qquad h_{ref}\left(s\right) \equiv \frac{1}{\rho_{ref}\left(s\right)}, \qquad \beta \equiv \frac{v}{c} \tag{2}$$

[7] Using the same dynamical model for analytical- and numerical studies. In particular when lattice errors are included.

and t the *absolute time of flight.* ρ_{ref} is the local radius of curvature along the reference curve followed by the comoving frame[8]. The *momentum deviation*

$$\delta \equiv \frac{p - p_0}{p_0} \tag{3}$$

is introduced by the canonical transformation

$$\begin{aligned} F_2 &= \frac{ct}{\beta}\left[1 - \sqrt{1 + \beta^2\left(2\delta + \delta^2\right)}\right], \qquad H_2 = H_1 + \frac{\partial F_2}{\partial s} = H_1, \\ -cT &= \frac{\partial F_2}{\partial \delta} = -\frac{\beta\left(1+\delta\right)ct}{\sqrt{1 + \beta^2\left(2\delta + \delta^2\right)}}, \\ p_t &= \frac{\partial F_2}{\partial\left(ct\right)} = \frac{1}{\beta}\left[1 - \sqrt{1 + \beta^2\left(2\delta + \delta^2\right)}\right] \end{aligned} \tag{4}$$

leading to the Hamiltonian

$$\begin{aligned} H_2\left(x, p_x, y, p_y, \delta, ct; s\right) &= -\left[1 + h_{ref}\left(s\right)x\right] \\ &\times \left\{\frac{q}{p_0}A_s\left(s\right) + \sqrt{\left(1+\delta\right)^2 - \left[p_x - \frac{q}{p_0}A_x\left(s\right)\right]^2 - \left[p_y - \frac{q}{p_0}A_y\left(s\right)\right]^2}\right\} \end{aligned} \tag{5}$$

Note that T, formally defined as the conjugate coordinate to δ, is not equal to the *time of flight* t, now given by

$$t = T\frac{\sqrt{1 + \beta^2\left(2\delta + \delta^2\right)}}{\beta\left(1+\delta\right)} \tag{6}$$

2.2 The Expanded Hamiltonian

We now introduce a sequence of justifiable approximations with the goal to obtain a simple but still accurate dynamical model. In the *ultrarelativistic limit* when $\beta \to 1$

$$p_t \to -\delta, \qquad t \to T \tag{7}$$

[8]We emphasize that the reference curve is in theory completely arbitrary. From a practical point of view, it is chosen primarily from engineering considerations, in particular the shape of the ideal *closed orbit.* A corresponding magnetic guiding field with trajectories of proper geometrical shape for ideal initial conditions is then determined.

This limit will be assumed in the following.[9] Note that at low energies, it is more suitable to use the momentum conjugate to the time of flight t, i.e. the energy deviation p_t defined by eq. (2). The multipole expansion of the vector potential [4] in the source-free environment of the beam can for the piece-wise constant case[10] be written

$$\begin{aligned}
\frac{q}{p_0} A_x(s) &= 0, \qquad \frac{q}{p_0} A_y(s) = 0, \\
\frac{q}{p_0} A_s(s) &\equiv -\mathrm{Re} \sum_{n=1}^{\infty} \frac{1}{n} \left[i a_n(s) + b_n(s) \right] \left(r e^{i\varphi} \right)^n \\
&= -\mathrm{Re} \sum_{n=1}^{\infty} \frac{1}{n} \left[i a_n(s) + b_n(s) \right] (x + iy)^n. \qquad (8)
\end{aligned}$$

From the curl in the curvilinear system [38]

$$\begin{aligned}
B_x(s) &= \frac{1}{1 + h_{ref}(s)\, x} \frac{\partial A_y}{\partial s} - \frac{\partial A_s}{\partial y}, \\
B_y(s) &= \frac{h_{ref}(s)}{1 + h_{ref}(s)\, x} A_s + \frac{\partial A_s}{\partial x} - \frac{1}{1 + h_{ref}(s)\, x} \frac{\partial A_x}{\partial s}, \\
B_s(s) &= \frac{\partial A_x}{\partial y} - \frac{\partial A_y}{\partial x} \qquad (9)
\end{aligned}$$

one then obtains the corresponding fields

$$\begin{aligned}
B_y(s) + i B_x(s) &= -\frac{p_0}{q} \sum_{n=1}^{\infty} \left[i a_n(s) + b_n(s) \right] \left(r e^{i\varphi} \right)^{n-1} \\
&= -\frac{p_0}{q} \sum_{n=1}^{\infty} \left[i a_n(s) + b_n(s) \right] (x + iy)^{n-1} \qquad (10)
\end{aligned}$$

valid for $h_{ref}(s) = 0$. In the case of dipole magnets $n = 1$, there are two natural geometries from an engineering point of view. The above *Cartesian geometry*

$$\frac{q}{p_0} A_s(s) = -b_1(s)\, x \qquad (11)$$

and the *cylindrical*

$$\frac{q}{p_0} A_s(s) = -\frac{b_1(s)}{2} \frac{1 + h_{ref}(s)\, x}{h_{ref}(s)} \qquad (12)$$

[9] The electron energy for SLS is ≈ 2.1 GeV compared to a rest mass of only 0.511 MeV.
[10] Ignoring fringe fields.

In the latter case the curvature of the local reference frame is chosen so that

$$h_{ref}(s) = b_1(s) \equiv \frac{1}{\rho_b(s)} \tag{13}$$

which has a geometrical interpretation in the form[11]

$$\frac{q}{p_0} = -\frac{1}{(B\rho_b)_0} \tag{14}$$

known as the *magnetic rigidity*. For precise modeling of dipoles with gradients see [93] for technical details.

We now apply the *adiabatic approximation* by taking advantage of the fact that the synchrotron oscillations are in general much slower than the betatron oscillations.[12] The momentum deviation can in other words be viewed as a slowly varying parameter rather than a dynamical variable obeying a dynamical law so that the longitudinal motion decouples from the transverse. The Hamiltonian eq. (1) is then expanded to third order in the phase space variables but keeping the exact parametric dependence in δ

$$\begin{aligned} &H_3(x, p_x, y, p_y; s) \\ &= -[1 + h_{ref}(s)x]\left[1 + \delta - \frac{p_x^2 + p_y^2}{2(1+\delta)} + \frac{q}{p_0}A_s(s)\right] + O(4) \end{aligned} \tag{15}$$

For simplicity, we will assume that the magnetic lattice can be modeled by a piece-wise constant field consisting of dipoles with cylindrical geometry and quadrupoles and sextupoles with Cartesian geometry. This leads to

$$\begin{aligned} &H_4(x, p_x, y, p_y; s) \\ &= [1 + b_1(s)x]\frac{p_x^2 + p_y^2}{2(1+\delta)} - b_1(s)x\delta + \frac{b_1^2(s)}{2}x^2 \\ &\quad + \frac{b_2(s)}{2}\left(x^2 - y^2\right) + \frac{b_3(s)}{3}\left(x^3 - 3xy^2\right) + O(4) \end{aligned} \tag{16}$$

Since the local curvature $h_{ref}(s)$ is small for a "medium size" ring[13], higher order kinematical terms may be ignored, so that finally

[11]Sign convention for electrons for which a left handed coordinate system is more convenient.

[12]The tunes for SLS are: $\nu_x \approx 20$, $\nu_y \approx 8$, and $\nu_s \approx 0.01$.

[13]Roughly, lattices for which $1/\rho_b^2 \ll b_2$. For SLS: $\rho_b \approx 5$ m, and $b_2 \approx 3$ m^{-2}.

$$
\begin{aligned}
& H_5\left(x, p_x, y, p_y; s\right) \\
&= \frac{p_x^2+p_y^2}{2(1+\delta)} - b_1(s)\, x\delta + \frac{b_1^2(s)}{2} x^2 \\
&\quad + \frac{b_2(s)}{2}\left(x^2-y^2\right) + \frac{b_3(s)}{3}\left(x^3-3xy^2\right) + O(4) \qquad (17)
\end{aligned}
$$

Note, the ignored terms, including the kinematical term

$$
h_{ref}(s)\,\frac{p_x^2+p_y^2}{2(1+\delta)} \qquad (18)
$$

may contribute significantly to the chromaticity in "small rings" [24, 25].

2.3 Hamilton's Equations

The equations of motion are obtained from Hamilton's equations

$$
\begin{aligned}
x' &\equiv \frac{dx}{ds} = \frac{\partial H_5}{\partial p_x} = \frac{p_x}{1+\delta} + O(3), \\
p'_x &\equiv \frac{dp_x}{ds} = -\frac{\partial H_5}{\partial x} \\
&= b_1(s)\,\delta - \left(b_1^2(s) + b_2(s)\right) x - b_3(s)\left(x^2-y^2\right) + O(3), \\
y' &\equiv \frac{dy}{ds} = \frac{\partial H_5}{\partial p_y} = \frac{p_y}{1+\delta} + O(3), \\
p'_y &\equiv \frac{dp_y}{ds} = -\frac{\partial H_5}{\partial y} = b_2(s)\, y + 2b_3(s)\, xy + O(3) \qquad (19)
\end{aligned}
$$

2.4 Symplectic Integration

The symplectic map generated by H_5 can be approximated by a *symplectic integrator*.[14] A second order symplectic integrator[15] is given by [70]

$$
S_2 \equiv e^{:-LH_5:} = e^{:-LH_{\text{drift}}/2:} e^{:-LH_{\text{kick}}:} e^{:-LH_{\text{drift}}/2:} + O\left(L^3\right) \qquad (20)
$$

[14] An integrator that preserves the internal symmetry of Hamilton's equations.

[15] A so called *kick code*.

where

$$
\begin{aligned}
H_{\mathrm{drift}} &= \frac{p_x^2 + p_y^2}{2\left(1+\delta\right)}, \\
H_{\mathrm{kick}} &= -b_1 x \delta + \frac{b_1^2}{2} x^2 + \frac{b_2}{2}\left(x^2 - y^2\right) + \frac{b_3}{3}\left(x^3 - 3xy^2\right)
\end{aligned}
\tag{21}
$$

In other words, each magnet is divided into a "drift-kick-drift". Moreover, it can be shown that, given a symplectic integrator of order $2n$, one may construct one of order $2n+2$ by [75]

$$
S_{2n+2}\left(L\right) = S_{2n}\left(z_1 L\right) S_{2n}\left(z_0 L\right) S_{2n}\left(z_1 L\right) + O\left(L^{2n+3}\right) \tag{22}
$$

where

$$
z_0 = -\frac{2^{1/(2n+1)}}{2 - 2^{1/(2n+1)}}, \qquad z_1 = \frac{1}{2 - 2^{1/(2n+1)}} \tag{23}
$$

A fourth order integrator is hence obtained by[16] [69, 70, 71, 72, 75]

$$
\begin{aligned}
e^{:-LH_1:} &= e^{:-c_1 L H_{\mathrm{drift}}:} e^{:-d_1 L H_{\mathrm{kick}}:} e^{:-c_2 L H_{\mathrm{drift}}:} e^{:-d_2 L H_{\mathrm{kick}}:} \\
&\quad \times e^{:-c_2 L H_{\mathrm{drift}}:} e^{:-d_1 L H_{\mathrm{kick}}:} e^{:-c_1 L H_{\mathrm{drift}}:} + O\left(L^5\right)
\end{aligned}
\tag{24}
$$

where

$$
\begin{aligned}
c_1 &= \frac{1}{2\left(2 - 2^{1/3}\right)}, \qquad c_2 = \frac{1 - 2^{1/3}}{2\left(2 - 2^{1/3}\right)}, \\
d_1 &= \frac{1}{2 - 2^{1/3}}, \qquad d_2 = -\frac{2^{1/3}}{2 - 2^{1/3}}
\end{aligned}
\tag{25}
$$

Note that while the second drift is "negative"

$$
2\left(c_1 + c_2\right) = 1, \qquad 2d_1 + d_2 = 1 \tag{26}
$$

as intuitively expected. The number of integration steps required to correctly model a given magnet are determined by numerical convergence of relevant computed quantities as usual, e.g. dynamical acceptance, but with the extra constraint that the tune should be kept constant. All tracking related to this work have been done with this model.

[16] Classical radiation is a straightforward modification of the kick [93].

The corresponding Taylor expanded transfer maps are obtained to arbitrary order by performing precisely the same arithmetic operations in TPSA. Computer implementations can therefore benefit substantially by using any modern object oriented language that supports operator overloading [26]. In fact, all numerical map and related normal form calculations used in the development and cross checking of the presented work have been performed by a beam line class,[17] with TPSA based on a polymorphic number class with reference counting [27], in C++.

2.5 (Generalized Hill's Equations)

For the sake of completeness, we also present the corresponding generalized Hill's equations. Note however, that they are never referred to in this work. In any case, they are obtained by combining Hamilton's equations into two second order ODEs. From eq. (19) one finds

$$\begin{aligned} x'' + \frac{b_2(s) + b_1^2(s)}{1+\delta} x &= b_1(s)\,\delta - \frac{b_3(s)}{1+\delta}\left(x^2 - y^2\right) + O(3)\,, \\ y'' - \frac{b_2(s)}{1+\delta} y &= \frac{2b_3(s)}{1+\delta} xy + O(3) \end{aligned} \tag{27}$$

3 Linear Beam Optics

3.1 Matrices: Element Description by Linear Symplectic Maps

The linear equations of motion are obtained from eqs. (19) for $b_3(s) = 0$

$$\begin{aligned} x' &= \frac{p_x}{1+\delta} + O(2)\,, \\ {p'}_x &= b_1(s)\,\delta - \left(b_1^2(s) + b_2(s)\right) x + O(2)\,, \\ y' &= \frac{p_y}{1+\delta} + O(2)\,, \\ {p'}_y &= b_2(s)\,y + 2b_3(s)\,xy + O(2) \end{aligned} \tag{28}$$

Integration leads to a linear transfer map representing a linear *coordinate transformation*

$$\vec{x}_1 = \vec{\xi}_{0\to1}(\vec{x}_0) = M_{0\to1}\vec{x}_0 \tag{29}$$

[17] J. Bengtsson and E. Forest unpubl.

where $M_{0\to1}$ is the well known 4×4 transfer matrix acting on the phase space vector $\vec{x} = [x, p_x, y, p_y]^T$. Concatenation is performed by ordinary matrix multiplication

$$M_{0\to2} = M_{1\to2} M_{0\to1} \tag{30}$$

The corresponding 4×4 matrices are easily determined by inspection from the traditional matrix formalism, see e.g. p. 12-14 in ref. [29], based on $\vec{x} = [x, x', y, y']^T$ since from eq. (28)

$$x' = \frac{p_x}{1+\delta}, \qquad y' = \frac{p_y}{1+\delta} \tag{31}$$

and the multipole components defined by eq. (8) have the momentum dependence

$$\frac{q}{p}A_s = \frac{q}{p_0}\frac{A_s}{1+\delta} \Rightarrow b_n(\delta) = \frac{b_n}{1+\delta} = (1+\delta+\cdots) \tag{32}$$

so that

$$\begin{bmatrix} x_1 \\ x'_{x1} \end{bmatrix} = \begin{bmatrix} m_{11} & m_{12} \\ m_{21} & m_{22} \end{bmatrix} \begin{bmatrix} x_0 \\ x'_{x0} \end{bmatrix} \quad \leftrightarrow \quad \begin{bmatrix} x_1 \\ p_{x1} \end{bmatrix} = \begin{bmatrix} m_{11} & \frac{m_{12}}{1+\delta} \\ m_{21}(1+\delta) & m_{22} \end{bmatrix} \begin{bmatrix} x_0 \\ p_{x0} \end{bmatrix} \tag{33}$$

These matrices are *symplectic*

$$MJM^T = J \tag{34}$$

where

$$J = \begin{bmatrix} 0 & 1 & 0 & 0 \\ -1 & 0 & 0 & 0 \\ 0 & 0 & 0 & 1 \\ 0 & 0 & -1 & 0 \end{bmatrix} \tag{35}$$

a reflection of the structure of Hamilton's equations as we shall see in section 4.1.

3.2 The δ-dependent Fix Point: Dispersion

The *linear dispersion function* $\vec{\eta}^{(1)}(s)$ is defined as the momentum dependent *fix point* of the linear one-turn map

$$M_{0\to n}\vec{\eta}^{(1)}(s_0)\,\delta \equiv \vec{\eta}^{(1)}(s_0)\,\delta \tag{36}$$

where

$$\vec{\eta}^{(1)}(s) \equiv \left[\eta_x^{(1)}(s), \eta'^{(1)}_x(s), \eta_y^{(1)}(s), \eta'^{(1)}_y(s)\right]^T \tag{37}$$

which is determined numerically by a closed orbit finder[18] since we have avoided to expand in δ. The fix point is translated to the origin of phase space by the transformation

$$\vec{x}(s) \to \vec{x}(s) + \vec{\eta}^{(1)}(s)\,\delta \tag{38}$$

3.3 Matrix Diagonalization: Global Properties

The one-turn matrix is diagonalized as usual

$$M_{0\to n} = A(s_0)\, R_{0\to n} A^{-1}(s_0) \tag{39}$$

where

$$R_{0\to n} = \begin{bmatrix} R_2(2\pi\nu_x) & [0] \\ [0] & R_2(2\pi\nu_y) \end{bmatrix}, \qquad R_2(\phi) = \begin{bmatrix} \cos\phi & \sin\phi \\ -\sin\phi & \cos\phi \end{bmatrix} \tag{40}$$

In the case of mid-plane symmetry[19] one finds, after imposing the Courant and Snyder choice for the phase advance, the unique (canonical) transformation [86]

$$A(s) = \begin{bmatrix} A_x(s) & [0] \\ [0] & A_y(s) \end{bmatrix}, \qquad A^{-1}(s) = \begin{bmatrix} A_x^{-1}(s) & [0] \\ [0] & A_y^{-1}(s) \end{bmatrix} \tag{41}$$

where

$$A_x(s) = \begin{bmatrix} \sqrt{\beta_x(s)} & 0 \\ -\frac{\alpha_x(s)}{\sqrt{\beta_x(s)}} & \frac{1}{\sqrt{\beta_x(s)}} \end{bmatrix}, \qquad A_x^{-1}(s) = \begin{bmatrix} \frac{1}{\sqrt{\beta_x(s)}} & 0 \\ \frac{\alpha_x(s)}{\sqrt{\beta_x(s)}} & \sqrt{\beta_x(s)} \end{bmatrix} \tag{42}$$

and similarly for the vertical plane.

The one-turn matrix at some arbitrary point k in the lattice is then given by

$$M_{k\to n+k} = M_{0\to k} M_{0\to n} M_{0\to k}^{-1} \tag{43}$$

[18]The Newton-Raphson method in multidimensions [28] is particularly suitable since the Jacobian is simply the one-turn matrix.

[19]No linear coupling. In the general case $A(s)$ will contain off-diagonal elements that have to be included to correctly determine what can be measured, i.e. the beam size.

However, it is sufficient to diagonalize $M_{0\to N}$ to determine the lattice functions at any arbitrary point since

$$\begin{aligned} M_{k\to n+k} &= A\left(s_k\right) R_{0\to k} R_{0\to n} R_{0\to k}^{-1} A^{-1}\left(s_k\right) \\ &= M_{0\to k} A\left(s_0\right) R_{0\to n} A^{-1}\left(s_0\right) M_{0\to k}^{-1} \end{aligned} \tag{44}$$

which leads to[20]

$$A\left(s_k\right) R_{0\to k} = M_{0\to k} A\left(s_0\right) \tag{45}$$

They are then computed directly from the matrix elements of $A\left(s_k\right) R_{0\to k}$ using

$$\begin{aligned} \alpha_x\left(s_k\right) &= -a_{11}\left(s_k\right) a_{21}\left(s_k\right) - a_{12}\left(s_k\right) a_{22}\left(s_k\right), \\ \beta_x\left(s_k\right) &= a_{11}^2\left(s_k\right) + a_{12}^2\left(s_k\right), \\ \Delta\mu_x &= \arctan\left(\frac{a_{12}\left(s_k\right)}{a_{11}\left(s_k\right)}\right) - \arctan\left(\frac{a_{12}\left(s_0\right)}{a_{11}\left(s_0\right)}\right), \\ \vec{\eta}^{(1)}\left(s_k\right) &= M_{0\to k}\vec{\eta}^{(1)}\left(s_0\right) \end{aligned} \tag{46}$$

All linear optics calculations required for this work has been done by this model.

4 Nonlinear Beam Dynamics

The following treatment is based on a paradigm shift currently taking place in nonlinear single particle beam dynamics [1, 3, 95]. It was actually conjectured in a paper by A.J. Dragt and J.M. Finn already back in 1976 [60]

> “It also provides a new approach since the connection between symplectic maps, Lie algebras, invariant functions, and Birkhoff’s work has not been previously recognized and exploited. It is expected that the results obtained will be applicable to the normal form problem in Hamiltonian mechanics, the use of the Poincaré section map in stability analysis, and the behavior of magnetic field lines in a toroidal plasma device.”

[20] Mathematically equivalent to the “Transformation of Twiss parameters” e.g. eq. [7,100] p. 16 in ref. [29]

Indeed, this suggestion has since long materialized.[21] Part of the elegance of the developments along these lines originates from the fact that, rather than Fourier expand as customary and consequently have to deal with infinite sums [32, 33],[22] one proceeds more directly to the desired goal. However, these techniques demand for an elementary knowledge of Lie algebra, in reality not much beyond the level of ordinary quantum mechanics, appears to have been a major obstacle for them to gain general acceptance. This is somewhat unfortunate, because one of the new techniques' major achievements is to bring nonlinear single particle dynamics back to the spirit of Courant and Snyder's by now[23] elementary linear stability analysis [20], based on the one-turn transfer matrix, i.e. the linear (symplectic) one-turn map.[24] To quote the Bologna school [84]:

> "We describe the motion of a particle in the lattice of a hadron accelerator using the formalism of symplectic maps. We revisit the Courant-Snyder's theory and we stress that the reduction to normal form of a symplectic map is just the natural generalization of the linear theory."

In particular after this field's long detour along more or less successful attempts to apply techniques initially developed, and hence more suitable, for celestial mechanics.[25] Roughly, the classical eigenvalue problem and its elegant solution by matrix diagonalization, is in a straightforward manner generalized by the introduction of a recursive algorithm that order by order transforms the nonlinear (symplectic) map into normal form [84, 86] from which the global properties then easily are extracted.

This approach is of course mathematically equivalent to the more traditional Hamiltonian perturbation theory [5], but far more effective when it comes to carrying out explicit calculations, rather than the customary "In principle..." for accelerators. Hence with the virtue to free analytical models from unnecessary and often radical oversimplifications, and at last allowing

[21] See for example ref. [3, 30, 63, 65, 72, 85, 86, 94, 95].

[22] Closed forms actually exists, see for example [34] (but the treatment is incorrect since the the perturbation of the angle variable was missed).

[23] The reader with a broad interest is invited to make a comparison with the corresponding developments in the closely related field of control theory over the last 40 years.

[24] The Courant-Snyder invariant is more generally known as the action variable in Hamiltonian dynamics: $2J_x = \frac{1}{\beta_x(s)}\left[x^2 + \left(\beta_x(s)\,p_x + \alpha_x(s)\,x^2\right)\right]$ [31].

[25] See for example [32, 33, 34, 35, 36, 37, 38, 39].

the accelerator physicist to construct more realistic models. We summarize our point of view by a modest quote from A. Chao [40]:

> "There is a theorem stating when you have only a partial knowledge of the solution to a differential equation and do not know what to do next, make a Fourier transformation."

4.1 Lie Algebraic Structure of Hamiltonian Dynamics

Hamilton's equations can be written in the *symplectic*[26] form[27]

$$\dot{\vec{x}} = -\left(\frac{\partial H}{\partial \vec{x}} J\right)^T \tag{47}$$

where

$$J = \begin{bmatrix} 0 & 1 & 0 & 0 & 0 & 0 \\ -1 & 0 & 0 & 0 & 0 & 0 \\ 0 & 0 & 0 & 1 & 0 & 0 \\ 0 & 0 & -1 & 0 & 0 & 0 \\ 0 & 0 & 0 & 0 & 0 & 1 \\ 0 & 0 & 0 & 0 & -1 & 0 \end{bmatrix} \tag{48}$$

Defining the *Poisson bracket*

$$[f(\vec{x}), g(\vec{x})] \equiv \sum_{i=1}^{n} \left[\frac{\partial f(\vec{x})}{\partial x_i}\frac{\partial g(\vec{x})}{\partial p_{xi}} - \frac{\partial f(\vec{x})}{\partial p_{xi}}\frac{\partial g(\vec{x})}{\partial x_i}\right] = \frac{\partial f(\vec{x})}{\partial \vec{x}} J \left[\frac{\partial g(\vec{x})}{\partial \vec{x}}\right]^T \tag{49}$$

allows one to write the total time derivative for any function $f(\vec{x}; s)$ of the phase space variables and "time" (s) by

$$\frac{df(\vec{x}; s)}{ds} = -[H, f(\vec{x}; s)] + \frac{\partial f(\vec{x}; s)}{\partial s} \tag{50}$$

and in the case of no explicit s-dependence

$$\frac{df(\vec{x})}{ds} = -[H, f(\vec{x})] \tag{51}$$

[26]From greek: intertwined, introduced by H. Weyl 1939.

[27]Goldstein's [5] notation is inconsistent since $\vec{x}$ is a contravariant- and $\frac{\partial H}{\partial \vec{x}}$ a covariant vector as correctly stated, but the latter should, correspondingly, be represented as the transpose (dual) vector in the formalism. A so called 1-form. See in particular p. 392.

which reduce to Hamilton's equations for $f(\vec{x})$ any of the phase space variables. Note that the Hamiltonian is simply the generator of an infinitesimal (symplectic) coordinate transformation. The Poisson bracket is invariant under a canonical transformation, e.g. to action-angle variables $\left[\overline{J}, \overline{\phi}\right]$

$$[f(\vec{x}),\ g(\vec{x})]_{\vec{x}} = \left[f\left(\overline{J}, \overline{\phi}\right),\ g\left(\overline{J}, \overline{\phi}\right)\right]_{[\overline{J}, \overline{\phi}]} \tag{52}$$

Moreover, it has the following three properties:

antisymmetric

$$[f(\vec{x}), g(\vec{x})] = -[g(\vec{x}), f(\vec{x})] \tag{53}$$

distributive

$$[af(\vec{x}) + bg(\vec{x}), h(\vec{x})] = a[f(\vec{x}), h(\vec{x})] + b[g(\vec{x}), h(\vec{x})] \tag{54}$$

Jacobi's identity

$$[f(\vec{x}), [g(\vec{x}), h(\vec{x})]] + [g(\vec{x}), [h(\vec{x}), f(\vec{x})]] + [h(\vec{x}), [f(\vec{x}), g(\vec{x})]] = 0 \tag{55}$$

which defines a *Lie algebra*

If we write the Poisson bracket in the Lie operator form

$$: f(\vec{x}) : g(\vec{x}) \equiv [f(\vec{x}), g(\vec{x})] \tag{56}$$

eq. (51) takes the form

$$\frac{df(\vec{x})}{ds} = - : H : f(\vec{x}) \tag{57}$$

It can be shown that the commutator of two Lie operators

$$\{: f(\vec{x}) :, : g(\vec{x}) :\} \equiv : f(\vec{x}) :: g(\vec{x}) : - : g(\vec{x}) :: f(\vec{x}) : \tag{58}$$

is homomorphic to the Poisson bracket

$$\{: f(\vec{x}) :, : g(\vec{x}) :\} \ \rightarrow : [f(\vec{x}), g(\vec{x})] : \tag{59}$$

In other words, that two Lie operators are equal

$$: f(\vec{x}) :=: g(\vec{x}) : \tag{60}$$

for any two functions that differ by an arbitrary constant a

$$f\left(\vec{x}\right)=g\left(\vec{x}\right)+a \tag{61}$$

As consequence, the Lie operators also form a Lie algebra.

Since the (functional) map for a Hamiltonian that commutes at different "times" (s)

$$\{: H\left(\vec{x},\ s_0\right):, : H\left(\vec{x},\ s_1\right):\}=0 \tag{62}$$

as a byproduct, it can be formally expressed in the form [62]

$$\mathcal{M}_{\vec{\xi}_{0\rightarrow1}}=\exp\left(:-\int_{s_0}^{s_1}H\left(s\right)ds:\right) \tag{63}$$

Roughly speaking, the problem of integrating the equations of motion has been reduced to algebraic manipulations by taking advantage of the underlying Lie algebraic structure of the Poisson bracket originating from Hamilton's equations.

As before, we now assume that each element can be represented by a piecewise constant Hamiltonian.[28] This is in general a good approximation for "medium-" and "large rings". When not, they are straightforward to include into the formalism [91]. Like for "small rings" or in interaction regions. The map for an element of length L is then simply

$$\mathcal{M}_{\vec{\xi}_{0\rightarrow1}}=\exp\left(:-LH:\right) \tag{64}$$

4.2 Element Description by Symplectic Maps

Each element is represented by a (functional) map $\mathcal{M}_{\vec{\xi}_{0\rightarrow1}}$ acting on functions $f\left(\vec{x}\right)$ of the *phase space* vector $\vec{x}=\left[x,p_x,y,p_y,\delta,ct\right]^T$

$$f\left(\vec{x}_1\right)=\mathcal{M}_{\vec{\xi}_{0\rightarrow1}}f\left(\vec{x}_0\right)\equiv f\circ\vec{\xi}_{0\rightarrow1}\left(\vec{x}_0\right) \tag{65}$$

with composition "$\circ$" defined by

$$f\circ\overline{\xi}_{0\rightarrow1}\left(\overline{x}_0\right)\equiv f\left(\overline{\xi}_{0\rightarrow1}\left(\overline{x}_0\right)\right) \tag{66}$$

[28] Ignoring fringe fields.

where $\vec{\xi}_{0\to1}(\vec{x}_0)$

$$\vec{x}_1 = \vec{\xi}_{0\to1}(\vec{x}_0) \tag{67}$$

is the corresponding transfer map.[29] Concatenation[30] is defined by

$$\mathcal{M}_{\vec{\xi}_{0\to1}} \mathcal{M}_{\vec{\xi}_{1\to2}} \equiv \mathcal{M}_{\vec{\xi}_{0\to2}} \tag{68}$$

We remark that it is of fundamental importance to have a conceptually clear understanding of these steps for the following treatment. For example, since

$$\begin{aligned} \mathcal{M}_{\vec{\xi}_{0\to2}} f &= \mathcal{M}_{\vec{\xi}_{1\to2}\circ\vec{\xi}_{0\to1}} f = f \circ \left(\vec{\xi}_{1\to2} \circ \vec{\xi}_{0\to1}\right) = \left(f \circ \vec{\xi}_{1\to2}\right) \circ \vec{\xi}_{0\to1} \\ &= \mathcal{M}_{\vec{\xi}_{0\to1}} \mathcal{M}_{\vec{\xi}_{1\to2}} f \end{aligned} \tag{69}$$

it follows that (functional) maps are concatenated in reversed order in contrast to transfer maps. These maps are said to be *symplectic* since the corresponding *Jacobian*

$$M_{0\to1} = \frac{\partial \vec{\xi}_{0\to1}(\vec{x}_0)}{\partial \vec{x}_0} \tag{70}$$

is a symplectic matrix, see eq. (34).

4.3 Parallel Transport and Lumping of Thin Kicks

The magnetic lattice is now separated into nonlinear thin kicks connected by linear maps. The one-turn map has then the following formal form [41]

$$\begin{aligned} \mathcal{M}_{\vec{\xi}_{0\to n}} &= \mathcal{M}_{\vec{\xi}_{0\to1}} e^{:V_1:} \mathcal{M}_{\vec{\xi}_{1\to2}} e^{:V_2:} ... e^{:V_{n-1}:} \mathcal{M}_{\vec{\xi}_{n-1\to n}} \\ &= \mathcal{M}_{\vec{\xi}_{0\to1}} e^{:V_1:} \mathcal{M}^{-1}_{\vec{\xi}_{0\to1}} \mathcal{M}_{\vec{\xi}_{0\to1}} \mathcal{M}_{\vec{\xi}_{1\to2}} e^{:V_2:} ... e^{:V_{n-1}:} \mathcal{M}^{-1}_{\vec{\xi}_{0\to n-1}} \mathcal{M}_{\vec{\xi}_{0\to n-1}} \mathcal{M}_{\vec{\xi}_{n-1\to n}} \\ &= e^{:\mathcal{M}_{\vec{\xi}_{0\to1}} V_1:} e^{:\mathcal{M}_{\vec{\xi}_{0\to2}} V_2:} ... e^{:\mathcal{M}_{\vec{\xi}_{0\to n-1}} V_{n-1}:} \mathcal{M}_{\vec{\xi}_{0\to n}} \\ &= \mathcal{A}_0^{-1} \mathcal{A}_0 e^{:\mathcal{M}_{\vec{\xi}_{0\to1}} V_1:} \mathcal{A}_0^{-1} \mathcal{A}_0 e^{:\mathcal{M}_{\vec{\xi}_{0\to2}} V_2:} ... \mathcal{A}_0^{-1} \mathcal{A}_0 e^{:\mathcal{M}_{\vec{\xi}_{0\to n-1}} V_{n-1}:} \mathcal{A}_0^{-1} \mathcal{R}_{0\to n} \mathcal{A}_n \\ &= \mathcal{A}_0^{-1} e^{:\widehat{V}_1:} e^{:\widehat{V}_2:} ... e^{:\widehat{V}_{n-1}:} \mathcal{R}_{0\to n} \mathcal{A}_n \end{aligned} \tag{71}$$

where we have introduced

$$\widehat{V}_i \equiv \mathcal{A}_0 \mathcal{M}_{\vec{\xi}_{0\to i}} V_i = \mathcal{R}_{0\to i} \mathcal{A}_i V_i \tag{72}$$

[29] A *coordinate transformation.* Precisely what *tracking codes* evaluates by direct numerical integration of the corresponding equations of motion. Eqs. (19) in our case.

[30] *Group multiplication.*

since for a similarity transformation

$$\mathcal{M} e^{:f:} \mathcal{M}^{-1} = e^{:\mathcal{M}f:} \tag{73}$$

whereas for linear maps

$$\mathcal{M}_{\vec{\xi}_{0\to i}} = \mathcal{A}_0^{-1} \mathcal{R}_{0\to i} \mathcal{A}_i \tag{74}$$

corresponding to eq. (45) in the matrix case. In other words, all the thin kicks have been parallel transported[31] to the beginning of the lattice.[32] They can now be lumped into a single thin kick by the Baker-Campbell-Hausdorff (BCH) theorem for noncommuting operators well known from elementary quantum mechanics

$$e^a e^b = e^{a+b+[a,\, b]/2+\dots} \tag{75}$$

so that finally

$$\begin{aligned} \mathcal{M}_{\vec{\xi}_{0\to n}} &\equiv \mathcal{A}_0^{-1} e^{:h:} \mathcal{R}_{0\to n} \mathcal{A}_n \\ &= \mathcal{A}_0^{-1} \exp\left(: \sum_{i=1}^{N} \widehat{V}_i + \frac{1}{2} \sum_{i<j}^{N} \left[\widehat{V}_i, \widehat{V}_j \right] + \cdots : \right) \mathcal{R}_{0\to n} \mathcal{A}_n \end{aligned} \tag{76}$$

4.4 Map Normal Form: Global Properties

The global properties of the lattice in the general nonlinear case[33] are determined by transforming the map into normal form [86]

$$\begin{aligned} \mathcal{M}_{\vec{\xi}_{0\to n}} &\equiv \mathcal{A}_0^{-1} e^{:h(\overline{J},\overline{\phi}):} \mathcal{R}_{0\to n} \mathcal{A}_0 \stackrel{?}{=} \mathcal{A}_0^{-1} e^{:-g(\overline{J},\overline{\phi}):} e^{:k(\overline{J}):} \mathcal{R}_{0\to n} e^{:g(\overline{J},\overline{\phi}):} \mathcal{A}_0 \\ &= \mathcal{A}_0^{-1} e^{:-g:} e^{:k:} e^{:\mathcal{R}_{0\to n} g:} \mathcal{R}_{0\to n} \mathcal{A}_0 \\ &= \mathcal{A}_0^{-1} e^{:k-(1-\mathcal{R}_{0\to n})g+[k,g]/2+[k-g,\mathcal{R}_{0\to n}g]/2+\cdots:} \mathcal{R}_{0\to n} \mathcal{A}_0 \end{aligned} \tag{77}$$

so that to first order

$$h^{(1)} = k^{(1)} - (1 - \mathcal{R}_{0\to n})\, g^{(1)} \tag{78}$$

[31] Compare with a space translation of a spinning top.

[32] Recall that (functional) maps acts in reversed order.

[33] In particular amplitude dependent tune shift, chromaticity and the lattice functions parametric dependence on δ and multipole strengths. The "unlocking of Pandora's box" for reasons that will become clear in the following.

To solve this equation h has to be decomposed into two parts: one part independent of the angle variables[34] and the remaining

$$h^{(1)} = h^{(1)}_{\mathrm{Ker}}\left(\overline{J}\right) + h^{(1)}_{\mathrm{Im}}\left(\overline{J}, \overline{\phi}\right) \tag{79}$$

so that

$$k^{(1)} = h^{(1)}_{\mathrm{Ker}}\left(\overline{J}\right), \qquad g^{(1)} = -\frac{1}{1-\mathcal{R}_{0\to n}} h^{(1)}_{\mathrm{Im}}\left(\overline{J}, \overline{\phi}\right) \tag{80}$$

which leads to

$$\begin{aligned} e^{:h:}\mathcal{R}_{0\to n} &= e^{:-g\left(\overline{J},\overline{\phi}\right):} e^{:k\left(\overline{J}\right):} \mathcal{R}_{0\to n} e^{:g\left(\overline{J},\overline{\phi}\right):} \\ &= e^{:\frac{1}{1-\mathcal{R}_{0\to n}} h^{(1)}_{\mathrm{Im}} \cdots :} \mathcal{R}_{0\to n} e^{:h^{(1)}_{\mathrm{Ker}} + h^{(2)}_{\mathrm{Ker}} - \frac{1}{2}\left[h^{(1)}_{\mathrm{Im}}, \frac{1}{1-\mathcal{R}_{0\to n}} h^{(1)}_{\mathrm{Im}}\right]_{\mathrm{Ker}} \cdots :} \\ &\quad \times e^{:-\frac{1}{1-\mathcal{R}_{0\to n}} h^{(1)}_{\mathrm{Im}} \cdots :} \end{aligned} \tag{81}$$

where $\left[\overline{J}, \overline{\phi}\right] \equiv [J_x, \phi_x, J_y, \phi_y]$ are the action-angle variables. This can strictly speaking only be done for integrable Hamiltonians.[35] In other words Hamiltonian systems without chaos. This is typically far from reality in the case of accelerators. However, the main goal of accelerator design, from a mathematical point of view, is to determine a design with a fix point surrounded by regular motion over an extensive volume of phase space. In other words, to avoid chaos. It is hence reasonable to assume that if one expands in some smallness parameter, e.g. the multipole strength, and brings the map perturbatively into normal form, the corresponding power series expansions should be able to model the dynamics in the regular regions of phase space. However, it can be shown that these expansions are only semiconvergent.[36] In any case, such a hypothesis can and should of course always be tested against tracking.

The tune shift is then easily obtained from the generator $k\left(\overline{J}\right)$ by

$$\Delta\nu_x = -\frac{1}{2\pi}\frac{\partial k\left(\overline{J}\right)}{\partial J_x}, \qquad \Delta\nu_y = -\frac{1}{2\pi}\frac{\partial k\left(\overline{J}\right)}{\partial J_y} \tag{82}$$

[34] The so called kernal of $\mathcal{R}_{0\to n}$, i.e. h for which $\mathcal{R}_{0\to n} h\left(\overline{J}\right) = 0$.

[35] Hamiltonian systems for which the motion is quasi-periodic and lies on a n-dimensional invariant torus in the $2n$-dimensional phase space.

[36] Generally known as the "small denominator problem".

whereas the canonical transformation $\exp(:g:)$ determines the distortions of the invariant torus. For example

$$\begin{aligned}\beta_{xi}+\Delta\beta_{xi} &= \left\langle e^{:g:}\mathcal{R}_{n\to i}\mathcal{A}_i x^2\right\rangle_{\overline{\phi}} = \beta_{xi}\left\langle e^{:g:}\mathcal{R}_{n\to i}x^2\right\rangle_{\overline{\phi}} \\ &= \beta_{xi}\left\langle (1+:g:+\cdots)\,\mathcal{R}_{n\to i}x^2\right\rangle_{\overline{\phi}} \qquad (83)\end{aligned}$$

where "$\langle\rangle_{\overline{\phi}}$" denotes averaging over the angle variables $[\phi_x,\phi_y]$.

5 Application to Sextupoles

In the following will work out analytical formula for various dynamical quantities as expansions in the multipole strength. *Order* will hence refer to order in multipole strength and NOT order in the phase space variables.[37]

5.1 Lie Generators: The Driving Terms

The vector potential for a thin sextupole at an arbitrary location s_i is

$$V_i = \frac{q}{p_0}A_s(s_i) = -\frac{b_{3i}}{3}\left(x^3-3xy^2\right) \qquad (84)$$

Noting that

$$\mathcal{A}_i x = \sqrt{\beta_{xi}}x + \eta_{xi}^{(1)}\delta \qquad (85)$$

one finds

$$\begin{aligned}\frac{1}{3}\mathcal{A}_i\left(x^3-3xy^2\right) &= \frac{1}{3}\left(\sqrt{\beta_{xi}}x+\eta_{xi}^{(1)}\delta\right)^3 - \left(\sqrt{\beta_{xi}}x+\eta_{xi}^{(1)}\delta\right)\beta_{yi}y^2 \\ &= \sqrt{\beta_{xi}}\left(\eta_{xi}^{(1)}\right)^2 x\delta^2 + \frac{1}{3}\beta_{xi}^{3/2}x^3 - \sqrt{\beta_{xi}}\beta_{yi}xy^2 \\ &\quad + \left(\beta_{xi}x^2-\beta_{yi}y^2\right)\eta_{xi}^{(1)}\delta + O\left(\delta^3\right) \qquad (86)\end{aligned}$$

[37]For example, a second-order achromat refers to a single-pass system for which all second order terms in the corresponding Taylor expanded map have been zeroed. This corresponds to that the first order effects in sextupole strength have been canceled. We are in the following, from a general point of view, attempting to design a circular accelerator based on a magnetic lattice corresponding to a third-order achromat in the single pass case [64].

Introducing the *resonance basis*

$$h_x^{\pm} \equiv \sqrt{2J_x} e^{\pm i\phi_x} = \sqrt{2J_x}\cos\phi_x \pm i\sqrt{2J_x}\sin\phi_x = x \mp ip_x \tag{87}$$

in other words the eigenfunctions of the *rotation operator* $\mathcal{R}$

$$\mathcal{R}_{i\to j} h_x^{\pm} = \mathcal{R}_{i\to j}\sqrt{2J_x} e^{\pm i\phi_x} = \sqrt{2J_x} e^{\pm i(\phi_x + \mu_{i\to j,x})} = e^{\pm i\mu_{i\to j,x}} h_x^{\pm} \tag{88}$$

Correspondingly

$$\begin{aligned} x &= \sqrt{2J_x}\cos\phi_x = \frac{1}{2}\left(h_x^+ + h_x^-\right), \\ p_x &= -\sqrt{2J_x}\sin\phi_x = -\frac{1}{2i}\left(h_x^+ - h_x^-\right) \end{aligned} \tag{89}$$

In the spirit of eqs. (41,65-67) we obtain

$$\begin{aligned} \mathcal{R}_{0\to i}\mathcal{A}_i \frac{1}{3}\left(x^3 - 3xy^2\right) &= \mathcal{R}_{0\to i}\left[\sqrt{\beta_{xi}}\left(\eta_{xi}^{(1)}\right)^2 x\delta^2 + \frac{1}{3}\beta_{xi}^{3/2}x^3 - \sqrt{\beta_{xi}}\beta_{yi}xy^2 \right. \\ &\quad \left. + \left(\beta_{xi}x^2 - \beta_{yi}y^2\right)\eta_{xi}^{(1)}\delta\right] + O\left(\delta^2\right) \end{aligned} \tag{90}$$

and

$$\begin{aligned} \mathcal{R}_{0\to i}x &= \frac{1}{2}\mathcal{R}_{0\to i}\left(h_x^+ + h_x^-\right) = \frac{1}{2}\left(h_x^+ \mathrm{e}^{i\mu_{xi}} + \text{c.c.}\right), \\ \mathcal{R}_{0\to i}x^2 &= \frac{1}{4}\mathcal{R}_{0\to i}\left(h_x^+ + h_x^-\right)^2 = \frac{1}{4}\left(h_x^{+2}\mathrm{e}^{i2\mu_{xi}} + \text{c.c.} + 4J_x\right), \\ \mathcal{R}_{0\to i}x^3 &= \frac{1}{8}\left(h_x^{+3}\mathrm{e}^{i3\mu_{xi}} + 3h_x^{+2}h_x^-\mathrm{e}^{i\mu_{xi}} + \text{c.c.}\right), \\ \mathcal{R}_{0\to i}xy^2 &= \frac{1}{8}\left[h_x^+ h_y^{+2}\mathrm{e}^{i\left(\mu_{xi}+2\mu_{yi}\right)} + h_x^+ h_y^{-2}\mathrm{e}^{i\left(\mu_{xi}-2\mu_{yi}\right)} \right. \\ &\quad \left. + 2h_x^+ h_y^+ h_y^- \mathrm{e}^{i\mu_{xi}} + \text{c.c.}\right] \end{aligned} \tag{91}$$

Collecting the terms we find that the Lie generator $: h :$, the nonlinear driving terms, has to first order the following generic form in the resonance basis

$$h^{(1)} \equiv \sum_{\left|\overline{I}\right|=n} h_{\overline{I}} h_x^{+i_1} h_x^{-i_2} h_y^{+i_3} h_y^{-i_4} \delta^{i_5} \tag{92}$$

where $\overline{I} \equiv [i_1, i_2, i_3, i_4, i_5]$, $\left|\overline{I}\right| \equiv i_1 + i_2 + i_3 + i_4 + i_5$. It may be interpreted as a *mode expansion* with each mode driving betatron- or synchro-betatron resonances and are summarized below.

The algebraic manipulations required to push on to the second order are straightforward and preferable automated by computer algebra. The BCH-theorem eq. (76) was implemented in MATHEMATICA[38] to automatically grind out the generator to second order for an arbitrary multipole component. The resulting second order terms have the form

$$\begin{aligned} h^{(2)} &\equiv \frac{1}{2}\sum_{i<j}\left[\widehat{V}_i,\widehat{V}_j\right] \\ &\equiv \frac{1}{J_x^{\alpha}J_y^{\beta}}\sum_{|\overline{I}|=|\overline{J}|=n} h_{\overline{I}}h_{\overline{J}}h_x^{+(i_1+j_1)}h_x^{-(i_2+j_2)}h_y^{+(i_3+j_3)}h_y^{-(i_4+j_4)}\delta^{i_5+j_5} \end{aligned} \tag{93}$$

5.1.1 First Order Chromatic Terms

Quadrupoles will also contribute since from eq. (32)

$$V_i = \frac{b_2}{2\left(1+\delta\right)}\left(x^2-y^2\right) = \frac{b_2}{2}\left(1-\delta\right)\left(x^2-y^2\right)+O\left(\delta^2\right) \tag{94}$$

There are two terms that are independent of the phase variable

$$\begin{aligned} h_{11001} &= \frac{1}{4}\sum_{i=1}^{N}\left[(b_2L)_i - 2(b_3L)_i\eta_{xi}^{(1)}\right]\beta_{xi}+O\left(\delta^2\right), \\ h_{00111} &= -\frac{1}{4}\sum_{i=1}^{N}\left[(b_2L)_i - 2(b_3L)_i\eta_{xi}^{(1)}\right]\beta_{yi}+O\left(\delta^2\right) \end{aligned} \tag{95}$$

which drive the linear chromaticity, the initial reason for introducing sextupoles into the lattice. The remaining are

$$\begin{aligned} h_{20001} &= h_{02001}^{*} = \frac{1}{8}\sum_{i=1}^{N}\left[(b_2L)_i - 2(b_3L)_i\eta_{xi}^{(1)}\right]\beta_{xi}e^{i2\mu_{xi}}+O\left(\delta^2\right), \\ h_{00201} &= h_{00021}^{*} = -\frac{1}{8}\sum_{i=1}^{N}\left[(b_2L)_i - 2(b_3L)_i\eta_{xi}^{(1)}\right]\beta_{yi}e^{i2\mu_{yi}}+O\left(\delta^2\right), \\ h_{10002} &= h_{01002}^{*} = \frac{1}{2}\sum_{i=1}^{N}\left[(b_2L)_i - (b_3L)_i\eta_{xi}^{(1)}\right]\eta_{xi}^{(1)}\sqrt{\beta_{xi}}e^{i\mu_{xi}}+O\left(\delta^3\right) \end{aligned} \tag{96}$$

where $*$ denotes the complex conjugate. h_{20001} and h_{00201} drive synchro-betatron resonances and generate momentum dependence of the beta functions, whereas h_{10002} drive second order dispersion. Unfortunately, this is far

[38]L. Rivkin priv. comm.

from the end of the story. As we will see in the following, these terms are followed by a whole swamp of undesirable terms: "the unlocking of Pandora's box".

5.1.2 First Order Geometric Terms

$$
\begin{aligned}
h_{21000} &= h^*_{12000} = -\frac{1}{8}\sum_{i=1}^{N}(b_{3i}L)\,\beta_{xi}^{3/2}e^{i\mu_{xi}}, \\
h_{30000} &= h^*_{03000} = -\frac{1}{24}\sum_{i=1}^{N}(b_{3i}L)\,\beta_{xi}^{3/2}e^{i3\mu_{xi}}, \\
h_{10110} &= h^*_{01110} = \frac{1}{4}\sum_{i=1}^{N}(b_{3i}L)\,\beta_{xi}^{1/2}\beta_{yi}e^{i\mu_{xi}}, \\
h_{10020} &= h^*_{01200} = \frac{1}{8}\sum_{i=1}^{N}(b_{3i}L)\,\beta_{xi}^{1/2}\beta_{yi}e^{i(\mu_{xi}-2\mu_{yi})}, \\
h_{10200} &= h^*_{01020} = \frac{1}{8}\sum_{i=1}^{N}(b_{3i}L)\,\beta_{xi}^{1/2}\beta_{yi}e^{i(\mu_{xi}+2\mu_{yi})}
\end{aligned} \tag{97}
$$

These terms drive five different betatron modes with the frequencies:

$$
\nu_x,\ 3\nu_x,\ \nu_x - 2\nu_y,\ \nu_x + 2\nu_y \tag{98}
$$

which appears as the well known first order harmonics in the corresponding Fourier expanded expressions in the old-fashioned approach.

5.1.3 Second Order Chromatic Terms

The terms independent of the angle variables drive the second order chromaticity. But the related formula will be derived by a simpler approach, so they are not needed in the following analysis. The remaining terms drive the synchro-betatron sidebands of the first order resonances. However, since the first order betatron modes have to be canceled, they corresponding sidebands are expected to be weak and will be ignored in the following analysis.

5.1.4 Second Order Geometric Terms

The terms independent of the angle variables are

$$
\begin{aligned}
\left(h_{\bar{I}} h_{\bar{J}}\right)_{g,\mathrm{Ker}} &= -\frac{1}{64}\left(3h_{21000}h_{12000} + h_{30000}h_{03000}\right)(2J_x)^2 \\
&+ \frac{1}{16}\left(2h_{21000}h_{01110} + h_{10020}h_{01200} + h_{10200}h_{01020}\right)(2J_x)(2J_y) \\
&- \frac{1}{64}\left(4h_{10110}h_{01110} + h_{10020}h_{01200} + h_{10200}h_{01020}\right)(2J_y)^2 \quad (99)
\end{aligned}
$$

and drive amplitude dependent tune shift. These effects may be viewed as originating from an amplitude- or momentum dependent shift of the closed orbit in the sextupoles. The remaining terms are

$$
\begin{aligned}
&\left(h_{\bar{I}} h_{\bar{J}}\right)_{g,\mathrm{Im}} \\
&= \frac{1}{64}\left[2(h_{30000}h_{12000})_{2\nu_x} + (h_{30000}h_{21000})_{4\nu_x}\right](2J_x)^2 \\
&+ \frac{1}{64}\Big[2\left(h_{30000}h_{01110} + h_{21000}h_{10110} + 2h_{10200}h_{10020}\right)_{2\nu_x} \\
&+ 2\left(h_{10200}h_{12000} + h_{21000}h_{01200} + 2h_{10200}h_{01110} + 2h_{10110}h_{01200}\right)_{2\nu_y} \\
&+ \left(h_{21000}h_{10020} + h_{30000}h_{01020} + 4h_{10110}h_{10020}\right)_{2\nu_x - 2\nu_y} \\
&+ \left(h_{30000}h_{01200} + h_{10200}h_{21000} + 4h_{10110}h_{10200}\right)_{2\nu_x + 2\nu_y}\Big](2J_x)(2J_y) \\
&+ \frac{1}{64}\left[2\left(h_{10200}h_{01110} + h_{10110}h_{01200}\right)_{2\nu_y} + (h_{10200}h_{01200})_{4\nu_y}\right](2J_y)^2 \\
&+ \text{c.c.} \qquad (100)
\end{aligned}
$$

and drive 8 different betatron modes with the frequencies:

$$
2\nu_x,\ 4\nu_x,\ 2\nu_y,\ 4\nu_y,\ 2\nu_x - 2\nu_y,\ 2\nu_x + 2\nu_y \qquad (101)
$$

We note that the second order modes appears due to cross terms of the first order modes.

5.2 Phenomenology: Lattice Perturbations

Sections 5.1.1-5.1.4 presented the driving terms, i.e. the Hamiltonian. We will now compute the corresponding perturbations on the linear lattice functions. In other words, determine perturbative solutions[39] to the nonlinear equations of motion.

[39] Expanded in the multipole strength.

5.2.1 Linear Chromaticity

The linear chromaticity is obtained directly from $h_{\rm Ker}^{(1)}$

$$\xi_x^{(1)} \equiv \left.\frac{\partial \nu_x}{\partial \delta}\right|_{\delta=0} = -\frac{1}{2\pi}\frac{\partial h_{11001}}{\partial J_x}, \qquad \xi_y^{(1)} \equiv \left.\frac{\partial \nu_y}{\partial \delta}\right|_{\delta=0} = -\frac{1}{2\pi}\frac{\partial h_{00111}}{\partial J_y} \tag{102}$$

so that

$$\begin{aligned}\xi_x^{(1)} &= -\frac{1}{4\pi}\sum_{i=1}^{N}\left[(b_2L)_i - 2(b_3L)_i\eta_{xi}^{(1)}\right]\beta_{xi},\\ \xi_y^{(1)} &= \frac{1}{4\pi}\sum_{i=1}^{N}\left[(b_2L)_i - 2(b_3L)_i\eta_{xi}^{(1)}\right]\beta_{yi}\end{aligned} \tag{103}$$

5.2.2 First Order Perturbations of Lattice Functions

The one-turn map with a dipole perturbation b_{1n} at the end can be written

$$\begin{aligned}\mathcal{M}_{\vec{\xi}_{0\to n}} &= \mathcal{M}_{\vec{\xi}_{0\to n-1}} e^{:b_{1n}x:} = \mathcal{A}_0^{-1}\mathcal{R}_{0\to n}\mathcal{A}_0 e^{:b_{1n}x:} = \mathcal{A}_0^{-1}\mathcal{R}_{0\to n} e^{:b_{1n}\mathcal{A}_0 x:}\mathcal{A}_0\\ &= \mathcal{A}_0^{-1}\mathcal{R}_{0\to n} e^{:b_{1n}\left(\sqrt{\beta_{xn}}x+\eta_{xn}^{(1)}\delta\right):}\mathcal{A}_0\end{aligned} \tag{104}$$

More generally, the map with a dipole kick at an arbitrary location j observed at location i is then

$$\begin{aligned}\mathcal{M}_{\vec{\xi}_{i\to n+i}} &= \mathcal{M}_{\vec{\xi}_{j\to i}}^{-1}\mathcal{M}_{\vec{\xi}_{j\to n+j}}\mathcal{M}_{\vec{\xi}_{j\to i}}\\ &= \mathcal{A}_i^{-1}\mathcal{R}_{j\to i}^{-1}\mathcal{R}_{j\to n+j} e^{:b_{1j}\left(\sqrt{\beta_{xj}}x+\eta_{xj}^{(1)}\delta\right):}\mathcal{R}_{j\to i}\mathcal{A}_i\end{aligned} \tag{105}$$

which corresponds to eq. (43) in the matrix case. Using eqs. (80) and (81) to transform into normal form gives

$$\begin{aligned}g^{(1)} &= -\frac{1}{1-\mathcal{R}_{j\to n+j}}h_{\rm Im}^{(1)} = -\frac{1}{1-\mathcal{R}_{j\to n+j}}b_{1j}\sqrt{\beta_{xj}}x\\ &= -\frac{b_{1j}}{2}\sqrt{\beta_{xj}}\frac{1}{1-\mathcal{R}_{j\to n+j}}\left(h_x^+ + h_x^-\right)\\ &= -\frac{b_{1j}}{2}\sqrt{\beta_{xj}}\left(\frac{h_x^+}{1-e^{i2\pi\nu_x}} + \text{c.c.}\right)\end{aligned} \tag{106}$$

and

$$\mathcal{R}_{j\to i}\mathcal{A}_i x = \sqrt{\beta_{xi}}\mathcal{R}_{j\to i}x + \eta_{xi}\delta = \frac{1}{2}\sqrt{\beta_{xi}}\left(h^+ e^{i\mu_{x,j\to i}} + \text{c.c.}\right) + \eta_{xi}\delta \quad (107)$$

So similar to eq. (83), the change of the closed orbit is given by

$$\begin{aligned} x_{\text{cod},i} &= \langle e^{:g:}\mathcal{R}_{j\to i}\mathcal{A}_i x\rangle_{\overline{\phi}} = \langle (1+:g:+\cdots)\,\mathcal{R}_{j\to i}\mathcal{A}_i x\rangle_{\overline{\phi}} \\ &= \frac{b_{1j}\sqrt{\beta_{xi}\beta_{xj}}}{2\sin\pi\nu_x}\cos\left(\mu_{x,j\to i} - \pi\nu_x\right) + \eta_{xi}^{(1)}\delta, \quad i > j \end{aligned} \quad (108)$$

where we have used

$$\left[h^+, h^-\right] = 2i, \qquad \left[h^+, h^+\right] = \left[h^-, h^-\right] = 0 \quad (109)$$

The case $i < j$ is treated similarly and the general case is summarized by

$$x_{\text{cod},i} = \frac{\sqrt{\beta_{xi}}}{2\sin\pi\nu_x}\sum_{j=1}^{N} b_{1j}\sqrt{\beta_{xj}}\cos\left(|\mu_{x,i\to j}| - \pi\nu_x\right) + \eta_{xi}^{(1)}\delta \quad (110)$$

The second order dispersion $\eta^{(2)}$ is defined by

$$\eta_{xi}^{(2)} \equiv \frac{1}{2}\frac{\partial^2 x_{\text{cod},i}(\delta)}{\partial\delta^2}\bigg|_{\delta=0} = \frac{\partial\eta_{xi}(\delta)}{\partial\delta}\bigg|_{\delta=0} \quad (111)$$

Taking into account that the δ-dependence of the multipole component eq. (32) leads finally to

$$\begin{aligned} \eta_{xi}^{(2)} &= -\eta_{xi}^{(1)} + \frac{\sqrt{\beta_{xi}}}{2\sin(\pi\nu_x)}\sum_{j=1}^{N}\left[(b_2 L)_j - (b_3 L)_j \eta_{xj}^{(1)}\right] \\ &\quad \times \eta_{xj}^{(1)}\sqrt{\beta_{xj}}\cos\left(|\mu_{i\to j,x}| - \pi\nu_x\right) \end{aligned} \quad (112)$$

The same algebra can now be carried out for any multipole component and in particular a quadrupole error b_{2n}. Defining

$$\beta_{xi}^{(1)} \equiv \frac{\partial\beta_{xi}}{\partial\delta}\bigg|_{\delta=0}, \qquad \beta_{yi}^{(1)} \equiv \frac{\partial\beta_{yi}}{\partial\delta}\bigg|_{\delta=0} \quad (113)$$

for the beta-beat and eq. (83) leads similarly to

$$\begin{aligned} \beta_{xi}^{(1)} &= \frac{\beta_{xi}}{2\sin(2\pi\nu_x)}\sum_{j=1}^{N}\left[(b_2 L)_j - 2(b_3 L)_j\eta_{xj}^{(1)}\right]\beta_{xj}\cos\left(|2\mu_{i\to j,x}| - 2\pi\nu_x\right), \\ \beta_{yi}^{(1)} &= -\frac{\beta_{yi}}{2\sin(2\pi\nu_y)}\sum_{j=1}^{N}\left[(b_2 L)_j - 2(b_3 L)_j\eta_{xj}^{(1)}\right]\beta_{yj}\cos\left(|2\mu_{i\to j,y}| - 2\pi\nu_y\right) \end{aligned} \quad (114)$$

5.2.3 Correction of Perturbed Lattice Functions

Note the similarity of formula (112) and (114) to (4.7) in ref. [20] which describes closed orbit distortions due to magnet tolerances.[40] By analogy then, second order dispersion and beta-beat may be corrected locally in the same manner as closed orbit distortions whenever desired. In particular, by solving the linear system

$$A\overline{x} = \overline{b} \tag{115}$$

For example in the case of horizontal beta-beat, the matrix coefficients in the correlation matrix $\overline{A}$ for closed orbit distortions

$$a_{ij} = \frac{\sqrt{\beta_{xi}\beta_{xj}}}{2\sin(\pi\nu_x)}\cos(|\mu_{i\to j,x}| - \pi\nu_x) \tag{116}$$

is simply replaced by

$$a_{ij} = \frac{\beta_{xi}\beta_{xj}}{2\sin(2\pi\nu_x)}\cos\left(\left|2\mu_{i\to j,x}\right| - 2\pi\nu_x\right) \tag{117}$$

whereas the undetermined dipole kicks b_{1j} in the vector $\overline{x}$ are replaced by the sextupole kicks $-2(b_3L)_j\eta^{(1)}_{xj}$, and the right hand side by the negative contribution to the beta-beat at each observation point i due to the quadrupoles

$$-\frac{\beta_{xi}}{2\sin(2\pi\nu_x)}\sum_{j=1}^{N}(b_2L)_j\beta_{xj}\cos(|2\mu_{i\to j,x}| - 2\pi\nu_x) \tag{118}$$

However, engineering problems described by such systems of linear equations tend to be overdetermined and can only be solved in a least-square sense. Preferably by singular value decomposition (SVD), see section 6.2.1.

5.2.4 Second Order Amplitude Dependent Tune Shift

These formula were derived in the author's thesis [38] by application of time dependent perturbation theory [5] and computer algebra. The work was inspired by a first order treatment based on variation of constants by B. Autin in his pursuit of a sextupole scheme for ACOL at CERN, who also rederived them later [39]. They later prompted J. Irwin at the SSC to once again

[40] The integral is replaced by a sum in the case of thin kicks, and $y(s) = \eta(s)\beta(s)$, $f(\psi) = \beta^{3/2}(s)F(s)$, $\frac{d\psi}{ds} = \frac{1}{\nu\beta(s)}$

rederive them, but this time along the lines outlined by E. Forest [41, 42]. In fact, MACSYMA programs were developed to automatically generate a few thousand lines of FORTRAN code to form an analytical model able to predict the short term dynamics for the SSC. Simply put, hours of tracking on a CRAY were replaced by a few minutes of numerical evaluations of an analytical model on a VAX [30].

$$\begin{aligned}
\frac{\partial \nu_x}{\partial J_x} &= -\frac{1}{16\pi}\sum_{j=1}^{N}\sum_{k=1}^{N}(b_3L)_j(b_3L)_k\beta_{xj}^{3/2}\beta_{xk}^{3/2} \\
&\quad \times \left[\frac{3\cos\left(|\mu_{j\to k,x}|-\pi\nu_x\right)}{\sin\left(\pi\nu_x\right)}+\frac{\cos\left(|3\mu_{j\to k,x}|-3\pi\nu_x\right)}{\sin\left(3\pi\nu_x\right)}\right], \\
\frac{\partial \nu_x}{\partial J_y} &= \frac{\partial \nu_y}{\partial J_x} \\
&= \frac{1}{8\pi}\sum_{j=1}^{N}\sum_{k=1}^{N}(b_3L)_j(b_3L)_k\sqrt{\beta_{xj}\beta_{xk}}\beta_{yj}\left[\frac{2\beta_{xk}\cos\left(|\mu_{j\to k,x}|-\pi\nu_x\right)}{\sin\left(\pi\nu_x\right)}\right. \\
&\quad - \frac{\beta_{yk}\cos\left[|\mu_{j\to k,x}+2\mu_{j\to k,y}|-\pi\left(\nu_x+2\nu_y\right)\right]}{\sin\pi\left(\nu_x+2\nu_y\right)} \\
&\quad \left.+ \frac{\beta_{yk}\cos\left[|\mu_{j\to k,x}-2\mu_{j\to k,y}|-\pi\left(\nu_x-2\nu_y\right)\right]}{\sin\pi\left(\nu_x-2\nu_y\right)}\right], \\
\frac{\partial \nu_y}{\partial J_y} &= -\frac{1}{16\pi}\sum_{j=1}^{N}\sum_{k=1}^{N}(b_3L)_j(b_3L)_k\sqrt{\beta_{xj}\beta_{xk}}\beta_{yj}\beta_{yk}\left[\frac{4\cos\left(|\mu_{j\to k,x}|-\pi\nu_x\right)}{\sin\left(\pi\nu_x\right)}\right. \\
&\quad + \frac{\cos\left[|\mu_{j\to k,x}+2\mu_{j\to k,y}|-\pi\left(\nu_x+2\nu_y\right)\right]}{\sin\pi\left(\nu_x+2\nu_y\right)} \\
&\quad \left.+ \frac{\cos\left[|\mu_{j\to k,x}-2\mu_{j\to k,y}|-\pi\left(\nu_x-2\nu_y\right)\right]}{\sin\pi\left(\nu_x-2\nu_y\right)}\right] \qquad (119)
\end{aligned}$$

5.2.5 Second Order Chromaticity

The amount of algebra required to derive these formula can be reduced considerable by taking advantage of the fact that the driving terms were, at least in theory, not expanded in δ. The second order chromaticity may hence be calculated by considering the parameter dependence in the formula for linear chromaticity (95) with respect to δ:

$$
\begin{aligned}
\xi_x^{(2)} &\equiv \frac{1}{2}\frac{\partial^2 \nu_x(\delta)}{\partial \delta^2}\bigg|_{\delta=0} = \frac{1}{2}\frac{\partial}{\partial\delta}\frac{\partial \nu_x(\delta)}{\partial\delta}\bigg|_{\delta=0} \\
&= -\frac{1}{8\pi}\sum_{i=1}^{N}\left[\frac{\partial(b_2L)_i}{\partial\delta} - 2\frac{\partial(b_3L)_i}{\partial\delta}\eta_{xi}^{(1)}\right]\beta_{xi} \\
&+ \frac{1}{8\pi}\sum_{i=1}^{N}\left\{2(b_3L)_i\frac{\partial\eta_{xi}}{\partial\delta}\beta_{xi} - \left[(b_2L)_i - 2(b_3L)_i\eta_{xi}^{(1)}\right]\frac{\partial\beta_{xi}}{\partial\delta}\right\}\bigg|_{\delta=0}
\end{aligned} \tag{120}
$$

Since the multipole components have the δ dependence given by eq. (32) we obtain directly

$$
\begin{aligned}
\xi_x^{(2)} &= -\frac{1}{2}\xi_x^{(1)} + \frac{1}{8\pi}\sum_{i=1}^{N}\left\{2(b_3L)_i\eta_{xi}^{(2)}\beta_{xi} - \left[(b_2L)_i - 2(b_3L)_i\eta_{xi}^{(1)}\right]\beta_{xi}^{(1)}\right\}, \\
\xi_y^{(2)} &= -\frac{1}{2}\xi_y^{(1)} - \frac{1}{8\pi}\sum_{i=1}^{N}\left\{2(b_3L)_i\eta_{xi}^{(2)}\beta_{yi} + \left[(b_2L)_i - 2(b_3L)_i\eta_{xi}^{(1)}\right]\beta_{yi}^{(1)}\right\}
\end{aligned} \tag{121}
$$

The parameter dependence of the lattice functions is computed by formula (112) and (114) or numerical differentiation

$$
\begin{aligned}
\eta_x^{(2)} &= \frac{1}{2}\frac{\partial^2 x_{cod}(\delta)}{\partial\delta^2}\bigg|_{\delta=0} = \frac{1}{2}\frac{\partial\eta_x(\delta)}{\partial\delta}\bigg|_{\delta=0} \\
&= \frac{1}{2}\frac{x_{cod}(h) - 2x_{cod}(0) + x_{cod}(-h)}{h^2} + O\left(h^2\right) \\
&= \frac{1}{2}\frac{\eta_x(h) - \eta_x(-h)}{2h} + O\left(h^2\right), \\
\beta^{(1)} &= \frac{\partial\beta}{\partial\delta}\bigg|_{\delta=0} = \frac{\beta(h) - \beta(-h)}{2h} + O\left(h^2\right)
\end{aligned} \tag{122}
$$

Alternatively, $\xi^{(2)}$ may evaluated by direct numerical differentiation

$$
\begin{aligned}
\xi^{(2)} &= \frac{1}{2}\frac{\partial^2\nu(\delta)}{\partial\delta^2}\bigg|_{\delta=0} = \frac{1}{2}\frac{\partial\xi(\delta)}{\partial\delta}\bigg|_{\delta=0} \\
&= \frac{1}{2}\frac{\nu(h) - 2\nu(0) + \nu(-h)}{h^2} + O\left(h^2\right) \\
&= \frac{1}{2}\frac{\xi(h) - \xi(-h)}{2h} + O\left(h^2\right)
\end{aligned} \tag{123}
$$

6 Application to the Swiss Light Source (SLS)

At this point, we have prepared ourselves with a general linear model[41] for beam optics, based in particular on eqs. (29), (30), (33), (36), (38), (39), (45), (46). Moreover, a nonlinear model based on the expanded Hamiltonian eq. (17), the multipole expansion eq. (8), and numerical evaluation (tracking) using a 4th order symplectic integrator eq. (24).[42] More generally, a C++ implementation[43] allows us to perform the same numerical evaluations in Truncated Series Algebra (TPSA),[44] and extract the corresponding Taylor series one-turn maps to arbitrary order. A numerical implementation of the normal form algorithm also based on TPSA,[45] allows us to bring these maps into normal form eq. (77) and hence self-consistently[46] extract the global properties of the lattice to arbitrary order. Finally, an analytical model based on eqs. (71), (96), (97), (99), (100), (103), (112), (114), (119), (121) allows us to get a clear insight into the parameter dependence of the nonlinear driving terms and related dynamical quantities. Note that all the analytical results were obtained by purely algebraic manipulations, i.e. we never had to explicitly integrate the equations of motion eqs. (19). These formula have also been coded for fast numerical evaluation in terms of the linear lattice functions. In particular, Simpson's rule [28]

$$A = \int_0^h f(x)\,dx = \frac{h}{6}\left(f(0) + 4f\left(\frac{h}{2}\right) + f(h)\right) + O\left(h^5 \frac{\partial^4 f}{\partial x^4}\right) \qquad (124)$$

has been used to compute the contribution from quadrupoles, whereas one thin kick is sufficient to model the sextupoles in the SLS lattice. For efficiency, numerical differentiation according to formula (122) has been used to obtain the δ-dependence of the lattice functions, in particular $\partial\eta/\partial\delta$ and $\partial\beta/\partial\delta$. So, we are are finally ready to very carefully but deliberately open "Pandora's box".

[41] Not assuming mid-plane symmetry and not expanded in δ.

[42] The related computer implementation is based on H. Nishumura's idea to "modify" N. Wirth's Pascal-S compiler/interpreter [43, 44] enabling us to use Pascal as command language.

[43] The underlying beam line class was designed in collaboration with E. Forest.

[44] By interfacing to a FORTRAN library originally developed by M. Berz at SSC.

[45] By interfacing to a FORTRAN library developed by E. Forest together with the author.

[46] Using the same dynamical model for analytical- and numerical studies. In particular when lattice errors are included.

6.1 Elementary Design Considerations: Magnetic Lattice Symmetry

As any modern high performance synchrotron SLS has a magnetic lattice with very strong focusing and consequently large natural chromaticity.[47] This implies that the beam will occupy a fairly large area in the tune diagram. Since magnetic tolerances are unavoidable,[48] resonances will by definition be excited and affect the performance. Sextupoles are therefore added to cancel the leading order (linear) contribution. However, as we have already seen, this is far from the end of the story. In spectrometer design, high performance imaging systems are traditionally designed by imposing symmetry to cancel undesirable aberrations. There are essentially two different approaches [45].[49] The first, see e.g. [96], is to pair sextupoles with a matched phase advance of π. In other words, to group the sextupoles in pairs separated by the linear transfer matrix

$$M_{1\to 2} = \begin{bmatrix} -1 & 0 \\ 0 & -1 \end{bmatrix} \tag{125}$$

By such an overall arrangement, one may with two independent families of sextupoles cancel the linear chromaticities eqs. (103) driven by h_{11001} and h_{00111} eqs. (95), and all the first order geometric modes eqs. (97). However, this pattern may potentially systematically excite the first order chromatic modes h_{20001} and h_{00201} eqs. (96), in fact on a level comparable to h_{11001} and h_{00111}. Since they drive the beta-beat eqs. (114), they may generate a substantial amount of second order chromaticity eq. (121). Furthermore, the relatively wide separation of the sextupoles tend to make them relatively strong which may enhance the second order effects. In any case, practical space limitations makes such an approach academic for SLS. One may consider interleaved schemes, if care is taken to control the cross talk between the sextupoles, i.e. the second order terms [95].

The second approach is to design a *unit cell*, repeat it four or more times to create a macro cell, and adjust the total phase advance to 2π. The linear chromaticity and all the first order chromatic- as well as geometric modes are then canceled at the end of the structure. This approach was pursued

[47] The natural chromaticities for SLS are: $\xi_x^{(1)} \approx -75$, $\xi_y^{(1)} \approx -22$.

[48] On a fundamental level, pure magnetic dipoles and quadrupoles are inconsistent with Maxwell's equations.

[49] Brown is using order defined in terms of phase space variables.

successfully for the early SLS lattice. A lattice was constructed by repeating a unit cell with a phase advance of about $\nu_x = 0.4$ and $\nu_y = 0.1$ 5 times which and adding straight sections leading to a lattice with reasonable dynamical aperture. In particular after enlarging the number of sextupole families from two to six [10, 11]. However, the author could later prove this result an artifact caused by incorrect powering of the two chromatic families. Roughly, since the unit cell had a sextupole at each end, the first and the last sextupole of the macro cell should only be excited with half the strength. Indeed, the same performance could be obtained with only the original two chromatic families [12]. 4 phase trombones and more sextupole families still had to be added though, to be able to implement the desired flexibility of the lattice from a dynamical point of view [12]. This required 33 sextupole families to avoid breaking the symmetry of the lattice. A result that reflects a fundamental problem with this approach: how to introduce straight sections. Since the quadrupoles in the straight sections will also contribute to the natural chromaticity, their contribution has to be canceled nonlocally[50] by the chromatic sextupoles inside the macro cell, leading to a violation of the nice cancellation of the first order terms at the end of each macro cell. Obviously, one should at least maintain the global symmetry of the lattice to avoid unnecessary excitation of systematic resonances. Later, a lattice based on a TBA-structure was suggested, pursued and eventually finalized [13, 14]. The following presents work related to a systematic design towards its sextupole scheme. The importance of lattice symmetry can be appreciated by a glance at the formula for the first order geometric modes eqs. (97). It is clear that e.g. the sine terms of the driving terms disappears at any point with mirror symmetry in the lattice. It would in general take 5 additional independent[51] sextupole families to achieve the same result.

6.2 Linear Vector Spaces: 10 First Order Design Gauges

The first order generators for the geometric modes eqs. (97) and the chromatic eqs. (96) are sums of complex numbers. The contribution from each element may hence be represented as a vector in the complex plane. Include the horizontal- and vertical chromaticities and we end up with 18 numbers that ideally should be zeroed. However, this number is reduced to 10 at points

[50] Unless one can tolerate a sufficient amount of dispersion in the straights.

[51] Linearly independent from existing families, something far from trivial as we shall see.

with mirror symmetry in the lattice. Since these terms are linear in the sextupole strength, we have a linear system of equations

$$A\overline{x} = \overline{b} \tag{126}$$

where A is a $18 \times N_{b_3}$ matrix with the matrix elements

$$a_{ij} \sim \sum_{k \in N_j}^{N} \beta_{xk}^{(i_1+i_2)/2} \beta_{yk}^{(i_3+i_4)/2} \left(\eta_{xk}^{(1)}\right)^{i_5} e^{i\left[(i_1-i_2)\mu_{xk}+(i_3-i_4)\mu_{yk}\right]} \tag{127}$$

for N_{b_3} sextupole families, $\overline{x} = \left[(b_3L)_1, \cdots, (b_3L)_{N_{b_3}}\right]^T$ and $\overline{b}$ is a vector containing the excitations of the driving terms due quadrupoles

$$b_i \sim \sum_{k=1}^{N_{b_2}} (b_2L)_k \beta_{xk}^{(i_1+i_2)/2} \beta_{yk}^{(i_3+i_4)/2} \left(\eta_{xk}^{(1)}\right)^{j_5} e^{i\left[(i_1-i_2)\mu_{xk}+(i_3-i_4)\mu_{yk}\right]} \tag{128}$$

This system is likely to be overdetermined so we will use Singular Value Decomposition (SVD) to determine a solution in a least square sense.

6.2.1 SVD: How to Deal Effectively with Linear Equations

There are two essential aspects well worth knowing about matrices from a mathematical point of view: eigenvalues and singular values. The eigenvalue point of view is effectively both the foundation and beauty of the Courant and Snyder paper, and linear control theory in general for that matter. The singular values on the other hand are defined by the so called singular value decomposition (SVD) of a $M \times N$ matrix A into the product [28]

$$A = U\Sigma V^t \tag{129}$$

where U is a $M \times N$ column orthogonal matrix, U a $N \times N$ orthogonal matrix and Σ a $N \times N$ diagonal matrix with elements ≥ 0

$$\Sigma = \begin{bmatrix} \sigma_1 & 0 \\ 0 & \sigma_n \end{bmatrix} \tag{130}$$

where σ_i the singular values. The inverse is then simply

$$A^{-1} = V\Sigma^{-1}U^t \tag{131}$$

where

$$\Sigma^{-1} = \begin{bmatrix} \frac{1}{\sigma_1} & & 0 \\ & & \\ 0 & & \frac{1}{\sigma_n} \end{bmatrix} \tag{132}$$

The *rank* of the matrix is given by the number of singular values $\neq 0$. For numerical calculations it is useful to introduce the *condition number* defined as the ratio of the largest singular value to the smallest. A problem is said to be *ill-conditioned* if the reciprocal of the condition number is close to the floating point precision of the computer. The system of linear equations tends to be overdetermined in practical problems. In other words, one is dealing with a linear optimization problem

$$A\overline{x} = \overline{b} \tag{133}$$

such that the number of free parameters $x_1, ...x_N$ are less than the number of constraints $b_1, ...b_N$. One may then attempt to solve approximately, in particular in a least square sense

$$\chi^2 \equiv \left| A\overline{x} - \overline{b} \right|^2 \tag{134}$$

All that is needed for constructing the corresponding inverse matrix is to perform a SVD and replace reciprocal singular values above a certain magnitude by zero

$$\frac{1}{\sigma_i} \ \rightarrow \ 0 \tag{135}$$

This replacement incidentally also gives a unique solution with the smallest magnitude of $|\overline{x}|^2$ for underdetermined systems!

Note that the nonlinear case

$$\overline{f}\left(\overline{x}\right) = \overline{a} \tag{136}$$

may be treated similarly by taking a local point of view and linearizing

$$\overline{f}\left(\overline{x}_0 + \Delta\overline{x}\right) = \overline{f}\left(\overline{x}_0\right) + M\Delta\overline{x} + O\left(2\right) \tag{137}$$

where M is the Jacobian

$$M = \frac{\partial\overline{f}\left(\overline{x}\right)}{\partial\overline{x}} = \begin{bmatrix} \frac{\partial f_1}{\partial x_1} & \cdots & \frac{\partial f_1}{\partial x_N} \\ \vdots & & \vdots \\ \frac{\partial f_M}{\partial x_1} & \cdots & \frac{\partial f_M}{\partial x_N} \end{bmatrix} \tag{138}$$

like Newton-Raphson in multidimensions.

6.3 A Sextupole Scheme for the TBA Structure

So, by changing to a top down approach, a structure based on 12 TBAs and 12 straight sections was eventually found to potentially meet the tight requirements on the linear optics and, in particular with a sufficiently small emittance. A required introduction of at least two long straight sections could potentially reduce the periodicity to 2. One may intuitively argue then that high performance implies local correction, since only then is there little opportunity for the nonlinear perturbations to accumulate. Some preliminary studies on a lattice with four long- and 8 medium straights proved it feasible to cancel all the first order terms over three TBAs with 9 sextupole families, 4 chromatic and 5 geometric, and by tuning the phase advance close to $\Delta\nu_x = 4.75$ and $\Delta\nu_y = 1.75$ over 3 TBAs, i.e. from the center of a long straight section to the next. This choice of phase advance led to cancellation of the chromatic modes h_{20001} and h_{00201} over two such blocks. The constraints on the phase advance occurs since the 9 sextupole families are not independent. In fact, a Singular Value Decomposition (SVD) of the corresponding system of linear equations, see section 6.2.1, shows that the rank of the system is only 8; for 9 constraints: horizontal- and vertical chromaticity, 5 geometric- and 2 chromatic modes. This can be understood from eqs. (95) and (96). The driving term for horizontal chromaticity h_{11001} becomes linearly dependent to the chromatic mode h_{20001} when chromatic sextupoles from the same family are separated by $\Delta\nu_x \approx 0.5$. This is hard to avoid in a strongly focusing TBA cell, and was also the reason to introduce phase trombones in the earlier lattice. Short straights with a small value of the beta function, so called mini-betas, eventually also had to be accommodated. Since they tend to add a considerable amount of "nonlocal" chromaticity, their introduction into the lattice leads to a corresponding degradation in dynamical acceptance. In fact, after the first order terms have been canceled, the dynamical acceptance scales roughly with the square of the relative chromaticity

$$\widehat{\xi}_x \equiv \frac{\xi_x}{\nu_x}, \qquad \widehat{\xi}_y \equiv \frac{\xi_y}{\nu_y} \tag{139}$$

as one would naively expect if we are indeed limited by second order terms. The final lattice consists of a block with 1 long-, 1 medium-, and 2 short straights and a TBA between each which is repeated 3 times. In other words, a mirror symmetric lattice with periodicity 3. Furthermore, it has 12 sextupole families, 3 chromatic and 9 geometric, and a phase advance close to $\Delta\nu_x = 3.5$ and $\Delta\nu_y = 1.5$ over 2 TBAs. The rank of the corresponding system is of course 8 as before.

Note that the sextupoles should at least naively be placed where the linear optics functions have weak δ-dependence to avoid to generate second order chromaticity, see eqs. (112). Furthermore, the beam position monitors should be placed close[52] to the sextupoles, since an orbit in a sextupole will give a gradient error by feed-down which will globally perturb the beta function and phase advance, effectively reducing the symmetry of the lattice resulting in reduced performance. In other words, as long as the orbit is centered in the sextupoles dipole and quadrupole errors will be harmless to the dynamical acceptance, but the physical aperture is of course reduced since the equilibrium orbit is in general no longer at the center of the beam pipe.

6.4 Confronting the Second Order: Another 13 Design Gauges?

After having gained control over the first order terms, we are ready to confront the second order. An inventory gives from eqs. (100) 8 second order betatron modes, (119) second order horizontal- and vertical chromaticity, and (121) 3 terms for amplitude dependent tune shift. A total of 21 terms and 13 at points with mirror symmetry. Since the first order terms does not have to be strictly canceled, one may attempt a numerical optimization based on a merit function and attempts to determine suitable weights by tracking. In particular by the corresponding short term dynamical acceptance. However, one soon finds that the first order terms have to be fairly well canceled and that the second order terms are fairly stiff. Note that the second order modes appears due to cross terms of the first order, and one may conclude that local control of the first order terms is essential for controlling the second order.

[52] In terms of phase advance.

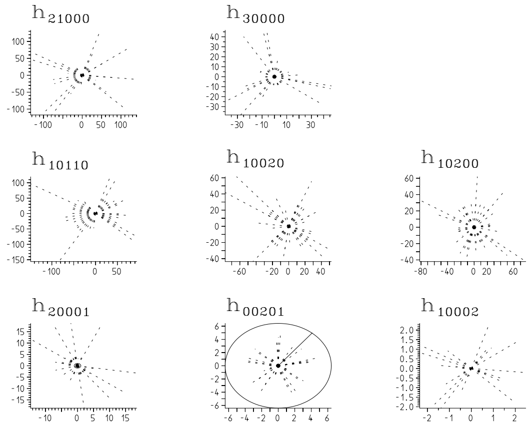

Figure 1: Zeroing of the First Order Modes.

6.5 So Where is the Cash?

Figure 1 shows a plot of the cancellation of the driving terms in the center of the medium straight. A circle indicates the residual amplitude. The chromatic mode h_{00201} is weakly excited due to other constraints related to the linear optics. Tracking for the initial conditions $J_x = 3.77 \times 10^{-6}, \phi_x = 0.0, J_y = 2.07 \times 10^{-6}, \phi_y = 0.0$ is shown in Figure 2. The unperturbed tunes are

$$\nu_x = 7.0800, \qquad \nu_x = 2.6400 \tag{140}$$

Fourier analysis of the horizontal and vertical position gives the actual tunes

$$\nu_x = 7.0906, \qquad \nu_x = 2.7189 \tag{141}$$

Fitting a linear combination of the betatron frequencies to the spurious peak in the horizontal plane

$$\nu = \nu_x - 2\nu_y = 1.6528 \approx 2 - 0.3471 = 1.6529 \tag{142}$$

and similarly for the vertical

$$\nu = 2\nu_x - \nu_y = 1.1462 \approx 1.4624 \tag{143}$$

It can be shown that it is a signal of the (amplitude) mode [38]

$$2\nu_x - 2\nu_x = k \tag{144}$$

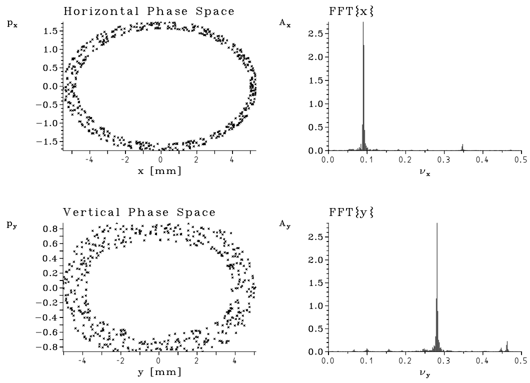

Figure 2: Tracking.

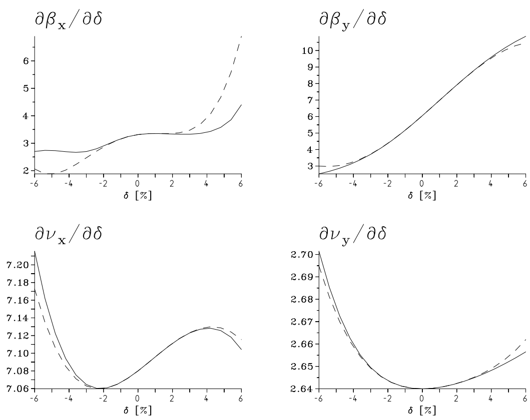

Figure 3: Chromatic Effects.

confirming that the first order modes have indeed been canceled. Figure 3 shows the chromatic effects where the solid line represents the computer model and the dashed the map normal form, i.e. perturbation theory. The linear horizontal chromaticity has been made positive to reduce

$$\xi_x = \left(\xi_x^{(1)} + \xi_x^{(2)}\delta + \cdots\right)\delta \tag{145}$$

rather than $\xi_x^{(1)}$. However, other considerations like the head-tail instability may impose other constraints. A numerical map normal form applied to an 7th order[53] one-turn map extracted by using a symplectic integrator and TPSA gives directly

$$\begin{aligned}
\beta_x(\delta) &= 3.32 + 8.88\delta - 6.18\times10^2\delta^2 + 8.72\times10^3\delta^3 \\
&\quad + 2.61\times10^5\delta^4 - 1.04\times10^7\delta^5 + O\left(\delta^6\right), \\
\beta_y(\delta) &= 6.05 + 9.17\times10^1\delta + 2.40\times10^2\delta^2 - 8.19\times10^3\delta^3 \qquad (146) \\
&\quad - 1.43\times10^4\delta^4 + 6.80\times10^5\delta^5 + O\left(\delta^6\right), \\
\xi_x(\delta) &= 7.08 + 1.50\delta + 1.35\times10^1\delta^2 - 5.49\times10^2\delta^3 \\
&\quad + 1.19\times10^3\delta^4 - 2.77\times10^4\delta^5 + O\left(\delta^6\right), \\
\xi_y(\delta) &= 2.64 - 5.06\times10^{-7}\delta + 7.08\delta^2 - 7.61\times10^1\delta^3 \\
&\quad + 9.96\times10^2\delta^4 - 1.06\times10^4\delta^5 + O\left(\delta^6\right) \qquad (147)
\end{aligned}$$

whereas a least square fit to the data gives

$$\begin{aligned}
\beta_x^*(\delta) &= 3.27 + 1.32\times10^1\delta - 3.43\times10^2\delta^2 - 5.29\times10^3\delta^3 \\
&\quad + 1.19\times10^5\delta^4 - 1.52\times10^7\delta^5 + O\left(\delta^6\right), \\
\beta_y^*(\delta) &= 6.05 + 9.16\times10^1\delta + 2.44\times10^2\delta^2 - 7.88\times10^3\delta^3 \\
&\quad - 1.82\times10^4\delta^4 + 4.82\times10^5\delta^5 + O\left(\delta^6\right), \\
\xi_x^*(\delta) &= 7.08 + 1.51\delta + 1.34\times10^1\delta^2 - 5.75\times10^2\delta^3 \\
&\quad + 2.46\times10^3\delta^4 - 2.83\times10^4\delta^5 + O\left(\delta^6\right), \\
\xi_y^*(\delta) &= 2.64 + 3.99\times10^{-3}\delta + 7.14\delta^2 - 8.55\times10^1\delta^3 \\
&\quad + 1.03\times10^3\delta^4 - 5.50\times10^3\delta^5 + O\left(\delta^6\right) \qquad (148)
\end{aligned}$$

[53] In the phase space variables.

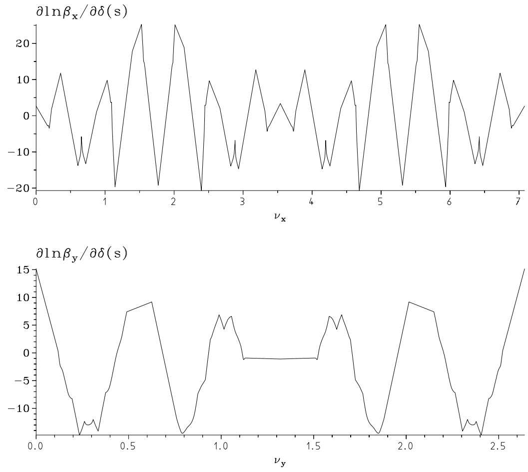

Figure 4: Relative Beta-Beat.

We conclude that perturbation theory works reasonable well within the boundary of regular motion. The poorer agreement in the horizontal plane is related to the fact that the linear optics is highly pushed in the horizontal plane whereas the vertical plane is more relaxed. Figure 4 and 5 shows the δ-dependence of the lattice functions around the lattice. We are plotting vs. ν_x, $2\nu_x$, and $2\nu_y$ since according to eq. (112) and (114) they are modulated with these frequencies. The dynamical acceptance with synchrotron oscillations and magnet misalignment errors[54] is presented in Figure 6. Indeed, by placing the BPMs close to sextupoles we essentially recover the dynamical acceptance.

7 The Experimentalist's Approach: In the Control Room

This section has been included for pedagogical reasons. In particular for followers of: "Everything in the control room is linear",[55] which clearly has more to do with definition than observation. For a model driven control

[54] An input file to impose correlations due to girders was written by A. Streun.

[55] There is a saying: "When reality outperforms our models, we instinctively prefer to ignore it rather than actively seek out how to raise our standards.".

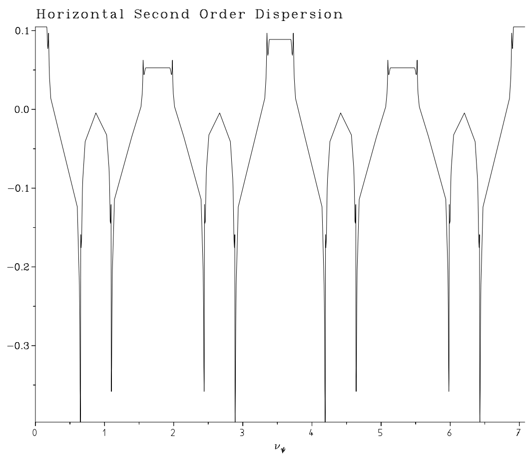

Figure 5: Second Order Dispersion.

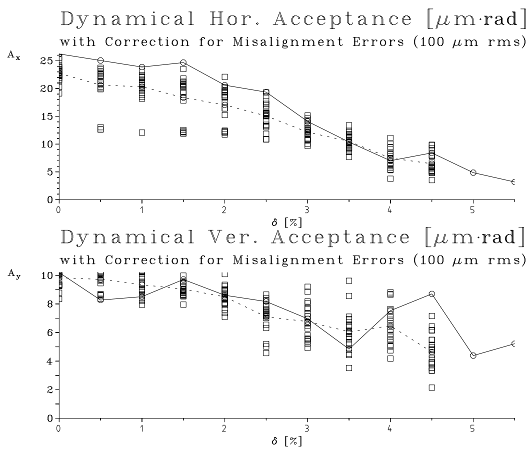

Figure 6: Dynamical Acceptance.

approach and related high precision measurements of the linear aspects, see for example ref. [38, 46, 47, 48, 49, 50].

7.1 The Perturbed Betatron Motion

One may represent a N-turn map as the one-turn raised map to N-th power. It is easily obtained from the one-turn map in its normal form eq. (77)

$$\begin{aligned}\mathcal{M}^N_{\vec{\xi}_{0\to n}} &= \mathcal{A}_0^{-1}\left(e^{:h\left(\overline{J},\overline{\phi}\right):}\mathcal{R}_{0\to n}\right)^N\mathcal{A}_0 \\ &= \mathcal{A}_0^{-1}e^{:-g\left(\overline{J},\overline{\phi}\right):}\left(e^{:k\left(\overline{J}\right):}\mathcal{R}_{0\to n}\right)^N e^{:g\left(\overline{J},\overline{\phi}\right):}\mathcal{A}_0 \\ &= \mathcal{A}_0^{-1}e^{:-g:}e^{:Nk:}\mathcal{R}^N_{0\to n}e^{:g:}\mathcal{A}_0 \end{aligned} \tag{149}$$

The perturbed betatron motion can now be determined. For example, the betatron mode $3\nu_x$ driven by h_{30000} in formula (97) has as generator

$$\begin{aligned} h^{(1)} &= h_{30000}h_x^{+3} + \text{c.c.} = A_{30000}e^{i\phi_{30000}}h_x^{+3} + \text{c.c.} \\ &= A_{30000}\left[\left(h_x^{+3} + \text{c.c.}\right)\cos\left(\phi_{30000}\right) + i\left(h_x^{+3} - \text{c.c.}\right)\sin\left(\phi_{30000}\right)\right] \\ &= 2A_{30000}(2J_x)^{3/2}\cos\left(3\phi_x + \phi_{30000}\right) \end{aligned} \tag{150}$$

where we have introduced

$$h_{30000} \equiv A_{30000}e^{i\phi_{30000}} \tag{151}$$

The perturbation of the action-angle variables $[J_x, \phi_x]$ is given by

$$J_x\left(N\right) = \mathcal{M}^N_{\vec{\xi}_{0\to n}}J_x, \qquad \phi_x\left(N\right) = \mathcal{M}^N_{\vec{\xi}_{0\to n}}\phi_x \tag{152}$$

and it follows that

$$\begin{aligned} J_x\left(N\right) &= e^{Nk}\mathcal{R}^N_{0\to n}\left(1 + :g: + \cdots\right)\mathcal{A}_0 J_x \\ &= e^{Nk}\mathcal{R}^N_{0\to n} : \left(1 - \frac{1}{1-\mathcal{R}_{0\to n}}h_{3\nu_x} + \cdots\right) : \mathcal{A}_0 J_x \\ &= \frac{A_{3\nu_x}}{2}\mathcal{R}^N_{0\to n} : \left[1 - \frac{h_x^{+3}e^{i\phi_{3\nu_x}}}{1-e^{i6\pi\nu_x}} + \text{c.c.}\right] : h_x^+h_x^- + O\left(b_3^2\right) \end{aligned} \tag{153}$$

By using

$$\left[h_x^{+3}, h_x^+h_x^-\right] = i6h_x^{+3} \tag{154}$$

we find in particular

$$\begin{aligned} J_x(N) &= J_x + \frac{3A_{3\nu_x}(2J_x)^{3/2}}{\sin(3\pi\nu_x)} \cos\left[\phi_{3\nu_x} + 3(\phi_x - \pi\nu_x + N2\pi\nu_x)\right] \\ &\quad + O\left(b_3^2\right) \end{aligned} \tag{155}$$

More generally, applying the same analysis to all the first order modes eqs. (97) gives

$$\begin{aligned} J_x(N) &= J_x + \frac{A_{21000}(2J_x)^{3/2}}{\sin(\pi\nu_x)} \cos\left(\widehat{\phi}_{21000} + \phi_x + N2\pi\nu_x\right) \\ &\quad + \frac{A_{10110}\sqrt{2J_x}2J_y}{\sin(\pi\nu_x)} \cos\left(\widehat{\phi}_{10110} + \phi_x + N2\pi\nu_x\right) \\ &\quad + \frac{3A_{30000}(2J_x)^{3/2}}{\sin(3\pi\nu_x)} \cos\left[\widehat{\phi}_{30000} + 3(\phi_x + N2\pi\nu_x)\right] \\ &\quad + \frac{A_{10020}\sqrt{2J_x}2J_y}{\sin[\pi(\nu_x - 2\nu_y)]} \cos\left[\widehat{\phi}_{10020} + \phi_x - 2\phi_y + N2\pi(\nu_x - 2\nu_y)\right] \\ &\quad + \frac{A_{10200}\sqrt{2J_x}2J_y}{\sin[\pi(\nu_x + 2\nu_y)]} \cos\left[\widehat{\phi}_{10200} + \phi_x + 2\phi_y + N2\pi(\nu_x + 2\nu_y)\right] \\ &\quad + O\left(b_3^2\right), \\ J_y(N) &= J_y - \frac{2A_{10020}\sqrt{2J_x}2J_y}{\sin[\pi(\nu_x - 2\nu_y)]} \cos\left[\widehat{\phi}_{10020} + \phi_x - 2\phi_y + N2\pi(\nu_x - 2\nu_y)\right] \\ &\quad + \frac{2A_{10200}\sqrt{2J_x}2J_y}{\sin[\pi(\nu_x + 2\nu_y)]} \cos\left[\widehat{\phi}_{10200} + \phi_x + 2\phi_y + N2\pi(\nu_x + 2\nu_y)\right] \\ &\quad + O\left(b_3^2\right) \end{aligned} \tag{156}$$

where

$$\widehat{\phi}_{ijkl0} \equiv \phi_{ijkl} - \pi\left[(i-j)\nu_x + (k-l)\nu_y\right] \tag{157}$$

7.2 DFT: Elementary Signal Processing

This section has been included to honor E. Asseo, a by now retired, electrical engineer in the LEAR group at CERN with a profound understanding of the Fourier transform and a deep passion for his programmable HP-calculator.

In fact, the whole experimental part of the author's thesis and related improvements of the stability of LEAR [38, 55, 57, 58] would not exist without his "Papy-Q" system (papy: french slang for grandpa) [56]. The versatility of his interpolation techniques for signal processing includes the conceptual design of the former SSC, see ref. [30], p. 119 [95]. Indeed, we are delighted to find that his work is currently being rediscovered [59]. The discrete Fourier transform (DFT) is defined by[56]

$$X_n \equiv \frac{1}{N}\sum_{k=0}^{N-1} x_k e^{-i2\pi k\Delta t n/N}, \qquad n = 0,\ 1,\ 2,\ \cdots,\ N-1 \tag{158}$$

where N is the number of samples, whereas Fast Fourier Transform (FFT) [54] is a fast algorithm to evaluate the transform for cases where $N = 2^k,\ k =$ integer. The amplitude distribution for a peak centered around the normalized frequency ν is given by

$$A_k = \left|\frac{\sin\left[\pi\left(k - N\nu\right)\right]}{\pi\left(k - N\nu\right)}\right| A_\nu, \qquad k = 0,\ 1,\ 2,\ \cdots,\ N-1 \tag{159}$$

The amplitude resolution can be improved by suppressing the sidelobes by folding the data with a weight function. For a sine window

$$x_k \to x_k \sin\frac{k\pi}{N}, \qquad 0 < k < N-1 \tag{160}$$

with the amplitude distribution

$$A_k = \frac{1}{2\pi}\left|\frac{\cos\pi\left(k - N\nu\right)}{\left(k - N\nu\right)^2 - \frac{1}{4}}\right| A_\nu, \qquad k = 0,\ 1,\ 2,\ \cdots,\ N-1 \tag{161}$$

Since the DFT is only defined for $\nu =$ integer so the frequency resolution is only in the order of $1/N$. However, the functional form for the amplitude distribution may be used to derive a nonlinear interpolation formula [55][57]

$$\nu^* = \frac{1}{N}\left[k - 1 + \frac{2A_k}{A_{k-1} + A_k} - \frac{1}{2}\right], \qquad k - 1 \le N\nu \le k \tag{162}$$

[56] For a so called rectangular window

[57] Exact for a single peak.

pushing the resolution to $1/N^2$ [59]. The amplitude can then be estimated from

$$A_\nu^* = \frac{2\pi\left[(k-N\nu)^2-\frac{1}{4}\right]}{\cos\pi\,(k-N\nu)}A_k \tag{163}$$

Note that the frequency resolution is also limited by the Nyquist criteria, i.e. the frequencies ν and $1-\nu$ can not be distinguished.[58] For the phase, the two samples on each side of the peak are separated by π with linear interpolation

$$\phi^* = \phi_k - N\,(\nu - k)\,\pi, \qquad k-1 \le N\nu \le k \tag{164}$$

in the case of a rectangular window.

7.3 A Purely Academic Exercise

We will now perform a purely academic exercise which has nothing to do with reality since we have so far only a conceptual design and no REAL accelerator, no control room, etc. And, the entire paper is too mathematical, too abstract and too theory oriented anyway. Simply put, too many equations... In any case, we will deliberately power three modes according to eqs. (165) and track a single particle for 512 turns and by Fourier analysis and elementary signal processing determine the corresponding amplitudes and phases in the frequency spectrum of the betatron motion. We deliberately excite the first order modes with the following values

$$\begin{aligned} A_{30000} &= 6.944, \quad \phi_{30000} = -1.8\,\text{deg},\\ A_{10020} &= 16.10, \quad \phi_{10020} = 54.0\,\text{deg},\\ A_{10200} &= 8.26, \quad \phi_{10200} = -70.2\,\text{deg} \end{aligned} \tag{165}$$

An easy calculation with formula (156) for the initial conditions

$$Jx = 1.5\times10^{-7}, \quad \phi_x = 0.0, \quad Jy = 1.0\times10^{-7}, \quad \phi_y = 90.0^\circ \tag{166}$$

gives the spectrum

f	A_x	ϕ_x	A_y	ϕ_y
$3\nu_x$	5.0×10^{-9}	-45.0 deg	–	–
$\nu_x-2\nu_y$	3.0×10^{-9}	90.0 deg	6.0×10^{-9}	-90.0 deg
$\nu_x+2\nu_y$	1.0×10^{-9}	45.0 deg	2.0×10^{-9}	45.0 deg

(167)

[58] So called *aliasing*. It is a reflection of the sampling theorem stating that to be able to resolve a frequency f one has to sample with at least $2f$.

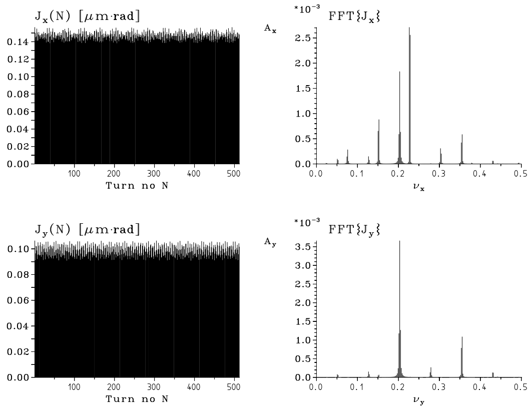

Figure 7: Perturbation of the Action Variables.

Figure 7 shows the tracking results. Fourier analysis and interpolation of the tracking data gives

$$\begin{array}{ccccc} f & A_x^* & \phi_x^* & A_y^* & \phi_y^* \\ 3\nu_x & 5.3\times10^{-9} & -45.1\,\mathrm{deg} & - & - \\ \nu_x-2\nu_y & 2.9\times10^{-9} & -82.6\,\mathrm{deg} & 5.8\times10^{-9} & 94.6\,\mathrm{deg} \\ \nu_x+2\nu_y & 1.0\times10^{-9} & 49.6\,\mathrm{deg} & 1.9\times10^{-9} & 49.0\,\mathrm{deg} \end{array} \tag{168}$$

The phase of $\nu = \nu_x - 2\nu_y$ appears with the wrong sign since it is $1-\nu$ that appears in the spectrum due to aliasing. Let us simply point out then, that one may in the control room measure the first order modes, compute the required increments in sextupole strength to obtain the same excitation (with a minus sign), and apply it as a correction to cancel the first order modes. Since we have already shown that the second order modes are driven by cross terms of the first order terms, their local cancellation effectively means indirect control of the second order. We have already illustrated what this means in terms of performance. The complementary aspect, how to measure and control the reduction of performance related to symmetry breaking due to engineering tolerances have already been operationally established, see ref. [38, 51, 52, 53].

8 Conclusions

We have summarized how modern techniques for single particle Hamiltonian dynamics allows one to easily implement an accurate and self-consistent computer model for numerical evaluation as well as analytical studies. A 4th order symplectic integrator that preserves the symplectic structure of Hamilton's equations allows for accurate long term tracking and extraction of the corresponding Taylor series maps to arbitrary order by replacing the related floating point arithmetic by Truncated Power Series Algebra (TPSA). Moreover, TPSA also makes it feasible to implement a map normal form algorithm to arbitrary order. The derivation of analytical formula to obtain insight into the parameter dependence of various dynamical properties is simplified considerable by taking advantage of the Lie algebraic structure of Hamilton's equations. These techniques allowed us to pursue a systematic design towards a sextupole scheme for the Swiss Light Source (SLS). In the process we also confirmed that perturbation theory works fairly well for the regions of phase space where the motion is regular, hence allowing us to model and reduce the effect of the nonlinear perturbations.

9 Acknowledgment

The author would like to thank W. Joho for general support and for teaching me how to improve my jogging skills (with C. Zaugg). The author would like to thank L. Rivkin for many stimulating beam dynamics discussions and physics discussions in general, and for many helpful suggestions when searching for references. The author would like to thank A. Streun for careful linear optics design and for upgrading his beam optics code to make it compatible with the author's computer model. In particular since the development of the sextupole scheme had to be interleaved with the linear optics development. The author would also like to thank him for porting procedures from the author into his code for second order terms as well as elementary signal processing. The author would finally like to thank G. Műlhaupt for his clear understanding of tolerances for accelerators, a general sense for priorities, and specially for having the courage to request a 6 months delay from the machine advisory committee and completely reopen the case before freezing the lattice, at a point when the earlier design had reached a level of complexity with 4 phase trombones and 33 sextupole families.

References

[1] H. Mais "Some Topics in Beam Dynamics of Storage Rings" DESY 96-119 (1996)

[2] A.J. Dragt "Summary of the Working Group on Maps" Part. Accel. vol. 55, pp. 253-284 (1996)

[3] E. Forest, L. Michelotti, A. Dragt, and J.S. Berg "Stability of Particle Motion in Storage Rings" Am. Inst. Phys. Proc. 292, pp. 417-487 (1994)

[4] J.D. Jackson "Classical Electrodynamics" (John Wiley & Sons, N.Y. 1975)

[5] H. Goldstein "Classical Mechanics" (Addison-Wesley, Reading, Mass. 1980)

[6] D.E. Knuth "The Art of Computer Programming" vol. 1 and 2 (Addison-Wesley, 1989)

[7] L.B. Rall "Automatic Differentiation: Techniques and Applications" Lecture Notes in Computer Science No. 120 (Springer-Verlag, 1981)

[8] G. Hori "Theory of General Perturbations with Unspecified Canonical Variables" Publ. Astron. Soc. Japan, vol. 18, pp. 287 (1966)

[9] A. Deprit "Canonical Transformations Depending on a Small Parameter" Celest. Mech. vol. 1, pp. 12-30 (1969)

The Swiss Light Source:

[10] "SLS Concept" PSI internal report Sept. 1993

[11] W. Joho, P. Marchand, L. Rivkin, and A. Streun "Design of a Swiss Light Source (SLS)" Fourth European Particle Accelerator Conference, June 27-July 1, 1994, London

[12] J. Bengtsson, W. Joho, P. Marchand, L. Rivkin, and A. Streun "Status of the Swiss Light Source Project SLS" Fifth European Particle Accelerator Conference, June 10-14, 1996, Barcelona

[13] "SLS-Handbook" PSI internal report Nov. 1996

[14] J. Bengtsson, W. Joho, P. Marchand, G. Muelhaupt, L. Rivkin, A. Streun "Increasing the Energy Acceptance of High Brightness Synchrotron Light Storage Rings" Nucl. Instr. Meth. vol. A404, pp. 237-247 (1998)

[15] M. Cornacchia "Lattices" pp. 30-58 (World Scientific, 1994) "Synchrotron Light Sources" H. Winick, ed.

[16] M.S. Zisman, S. Chattopadhyay, and J.J. Bisognano "ZAP User's Manual" LBL-21270 (1986)

[17] S. Khan "Simulation of the Touschek Effect for BESSY II — A Monto Carlo Approach" Fourth European Particle Accelerator Conference, June 27-July 1, 1994, London

[18] M. Meddahi, and J. Bengtsson "Studies of Transverse Coherent Bunch Instabilities for the Advanced Light Source (ALS)" LBL-35703 (1994)

[19] J. Bengtsson, D. Briggs, and M. Meddahi "Six-Dimensional Modeling of Coherent Bunch Instabilities and Related Feedback Systems in Storage Rings with Power-Series Maps for the Lattice" Fourth European Particle Accelerator Conference, June 27-July 1, 1994, London

[20] E.D. Courant and H.S. Snyder "Theory of the Alternating-Gradient Synchrotron" Ann. Phys. vol. 3, pp. 1-48 (1958)

[21] J. Bengtsson, D. Briggs, and G. Portmann "A Linear Control Theory Analysis of Transverse Coherent Bunch Instabilities Feedback Systems (The Control Theory Approach to Hill's Equation)" CBP Tech Note-026, PEP-II AP Note 28-93 (1993)

[22] J. Moser "Stable and Random Motion in Dynamical Systems" (Princeton University Press, 1973)

[23] I. Percival "Integrable and Nonintegrable Hamiltonian Systems" Lecture Notes In Physics 247 ed. J.M. Jowett, M. Month and S. Turner (Springer, 1986) p. 16

Chromaticity:

[24] J. Jäger and D. Möhl "Comparison of Methods to Evaluate the Chromaticity in LEAR" PS/DL/LEAR/Note 81-7 (1981)

[25] A.J. Dragt "Exact Numerical Calculation of Chromaticity in Small Rings" Part. Accel. vol. 12, pp. 205-218 (1982)

[26] L. Michelotti "MXYZPTLK: A Practical, User-Friendly C++ Implementation of Differential Algebra: User's Guide" FN-535 (1990)

[27] J.O. Coplien "Advanced C++: Programming Styles and Idioms" (Addison-Wesley, New York, 1992)

[28] W.H. Press, B.P. Flannery, S.A. Teukolsy, and W.T. Vetterling "Numerical Recipes" (Cambridge University Press, 1989)

[29] C. Bovet, R. Gouiran, I. Gumowski, K.H. Reich "A Selection of Formulae and Data Useful for the Design of A.G. Synchrotrons" CERN/MPS-SI/In. DL/70/4 (1970)

[30] J. Bengtsson and J. Irwin "Analytical Calculations of Smear and Tune Shift" SSC-232 (1990)

[31] R.D. Ruth "Single Particle Dynamics and Nonlinear Resonances in Circular Accelerators" Lecture Notes In Physics 247 ed. J.M. Jowett, M. Month and S. Turner (Springer, 1986) pp. 37-63

Perturbation Theory:

[32] A. Schoch "Theory of Linear and Non-linear Perturbations of Betatron Oscillations in Alternating Gradient Synchrotrons" CERN 57-21 (1957)

[33] G. Guignard "A General Treatment of Resonances in Accelerators" CERN 78-11 (1978)

[34] A. Ando "Distortion of Beam Emittance with Nonlinear Magnetic Fields" Part. Accel. vol. 15, pp. 177-207 (1984)

[35] L. Michelotti "Moser-like Transformations Using the Lie Transform" Part. Accel. vol. 16, pp. 233-252 (1985)

[36] L. Michelotti "Deprit's Algorithm, Green's Functions, and Multipole Perturbation Theory" Part. Accel. vol. 19, pp. 205-210 (1986)

[37] B. Autin "Nonlinear Betatron Oscillations" Am. Inst. Phys. Proc. 153 pp. 288-347 (1987)

[38] J. Bengtsson "Non-Linear Transverse Dynamics for Storage Rings with Applications to the Low-Energy Antiproton Ring (LEAR) at CERN" (thesis) CERN 88-05 (1988)

[39] B. Autin "Non-linear Betatron Oscillations" CERN 90-4 (1990)

[40] A.W. Chao "Physics of Collective Beam Instabilities in High Energy Accelerators" (John Wiley & Sons, N.Y. 1993)

[41] E. Forest "Analytical Calculation of the Smear" SSC-95 (1986)

[42] E. Forest "Computation of First Order Tune Shifts" SSC-N-322 (1987)

[43] R.E. Berry "Programming Language Translation" (John Wiley & Sons, N.Y., 1983)

[44] M. Rees and D. Robson "Practical Compiling with Pascal-S" (Addison-Wesley, N.Y., 1988)

[45] K.L. Brown and R.V. Servranckx "First- and Second-Order Charged Particle Optics" Am. Inst. Phys. Proc. 127 pp. 62-138 (1985)

Experimental Techniques:

[46] W.J. Corbett, M.J. Lee, and V. Ziemann "A Fast Model-Calibration Procedure for Storage Rings" SLAC-PUB-6111 (1993)

[47] J. Bengtsson and M. Meddahi "Elementary Analysis of BPM Data for the ALS Storage Ring" CBP Tech Note 003 (1993)

[48] M. Meddahi and J. Bengtsson "Study of Possible Energy Upgrade for the ALS and Modeling of the "Real Lattice" for the Diagnosis of Lattice Problems" 1993 Particle Accelerator Conference, Washington, DC, USA, May 17 - 20, 1993

[49] J. Bengtsson, W. Leemans and T. Byrne "Emittance Measurement and Modeling of the ALS 50 MeV Linac to Booster Line" 1993 Particle Accelerator Conference, Washington, DC, USA, May 17 - 20, 1993

[50] W. Fischer "An Experimental Study on the Long-Term Stability of Particly Motion in Hadron Storage Rings" (thesis) DESY 95-235 (1995)

Symmetry Restoration:

[51] J. Bengtsson and E. Forest "Global Matching of the Normalized Ring" Advanced Beam Dynamics Workshop on Effects of Errors in Accelerators, their Diagnosis and Corrections Corpus Christi, Texas, Oct. 3 - 8, 1991

[52] J. Bengtsson and M. Meddahi "Modeling of Beam Dynamics and Comparison with Measurements for the Advanced Light Source (ALS)" 4th European Particle Accelerator Conference - EPAC 94, London, UK, June 27 - July 1, 1994

[53] D. Robin, G. Portmann, H. Nishimura and J. Safranek "Model Calibration and Symmetry Restoration of the Advanced Light Source" Fifth European Particle Accelerator Conference, June 10-14, 1996, Barcelona

Discrete Fourier Transform Techniques:

[54] J.W. Cooley and J.W. Tukey "An Algorithm for the Machine Calculation of Complex Fourier Series" Math. of Comp. Vol. 19, pp. 297-301 (1965)

[55] E. Asseo "Moyens de Calcul pour la Mesure des Force et Phase des Effets perturbateurs des Résonances sur le Faisceau" CERN/PS/LEA Note 85-3 (1985)

[56] E. Asseo "Système Autosynchronisé pour la Mesure Automatique des Oscillations Bétatronique du Faisceau p ou $\bar{p}$" CERN/PS/LEA Note 87-1 (1985)

[57] E. Asseo, J. Bengtsson and M. Chanel "LEAR Beam Stability Improvements Using FFT Analysis" EPAC - 1st European Particle Accelerator Conference, Rome, Italy, 7 - 11 Jun 1988

[58] E. Asseo, J. Bengtsson and M. Chanel "Absolute and High Precision Measurements of Particle Beam Parameters at CERN Antiproton Storage Ring LEAR Using Spectral Analysis with Correction Algorithms" EUSIPCO-88: 4th European Signal Processing Conference, Grenoble, France, 5 - 8 Sep 1988

[59] R. Bartolini, M. Givannozzi, W. Scandale, A. Bazzani and E. Todesco "Algorithms for a Precise Determination of the Betatron Tune" Fifth European Particle Accelerator Conference, June 10-14, 1996, Barcelona

Basic Lie Algebraic Techniques for Accelerators:

[60] A.J. Dragt and J.M. Finn "Lie Series and Invariant Functions for Analytic Symplectic Maps" J. Math. Phys. Vol. 17, No. 12, pp. 2215-2227 (1976)

[61] A.J. Dragt "A Method of Transfer Maps for Linear and Nonlinear Beam Elements" IEEE Trans. Nucl. Sci. vol. NS-26, No. 3, pp. 3601-3603 (1979)

[62] "Lectures on Nonlinear Orbit Dynamics" Am. Inst. Phys. Proc. 87, pp. 147-313 (1982)

[63] A.J. Dragt, L.M. Healy, F. Neri, and R.D. Ryne "MARYLIE 3.0 - A Program for Nonlinear Analysis of Accelerator and Beamline Optics" IEEE Trans. Nucl. Sci. vol. NS-32, No. 5, pp. 2311-2313 (1985)

[64] A.J. Dragt "Elementary and Advanced Lie Algebraic Methods with Applications to Accelerator Design, Electron Microscopes, and Light Optics" Nucl. Instr. Meth. vol. A258, pp. 339-354 (1987)

[65] A.J. Dragt, F. Neri, G. Rangarajan, D.R. Douglas, L.M. Healy, and R.D. Ryne "Lie Algebraic Treatment of Linear and Nonlinear Beam Dynamics" Ann. Rev. Nucl. Part. Sci. vol. 38, pp. 455-496 (1988)

Generating Function Techniques:

[66] D.R. Douglas and A.J. Dragt "Lie Algebraic Methods for Particle Tracking Calculations" Proceedings of the 12th International Conference on High Energy Accelerators, F.T. Cole *et al.* (eds.), Fermilab (1983)

[67] D. Douglas and A. Dragt "MARYLIE, The Maryland Lie Algebraic Beam Transport and Particle Tracking Program" IEEE Trans. Nucl. Sci. vol. NS-30, No. 4, pp. 2442-2444 (1983)

[68] M. Berz "The Description of Particle Accelerators Using High-Order Perturbation Theory on Maps" Am. Inst. Phys. Proc. 184, pp. 961-994 (1989)

Symplectic Integrators:

[69] R.D. Ruth "A Canonical Integration Technique" IEEE Trans. Nucl. Sci. vol. NS-30, pp. 2669-2671 (1983)

[70] F. Neri "Lie Algebras and Canonical Integration" Unpubl. Maryland (1987)

[71] E. Forest "Lie Algebraic Maps and Invariants Produced by Tracking Codes" SSC-78 (1986)

[72] E. Forest and R.D. Ruth "Fourth-Order Symplectic Integration" Physica D 43, pp. 105-117 (1990)

[73] E. Forest "High-Order Description of Accelerators Using Differential Algebra and First Applications to the SSC" SSC-N-571 (1988)

[74] M. Suzuki "Fractal Decomposition of Exponential Operators with Applications to Many-Body Theories and Monto Carlo Simulations" Phys. Lett. A146, no. 6, pp. 319-323 (1990)

[75] H. Yoshida "Construction of Higher Order Symplectic Integrators" Phys. Lett. A 150, pp. 262-268 (1990)

[76] M. Suzuki "General Theory of Fractal Path Integrals with Applications to Many-Body Theories and Statistical Physics" J. Math. Phys. vol. 32, pp. 400-407 (1991)

[77] E. Forest, J. Bengtsson and M.F. Reusch "Application of the Yoshida-Ruth Techniques to Implicit Integration and Multi-Map Explicit Integration" Phys. Lett. A158 pp. 99-101 (1991)

Automatic Differentiation:

[78] M. Berz "The Method of Power Series Tracking for the Mathematical Description of Beam Dynamics" Nucl. Instr. Meth. vol. A258, pp. 431-436 (1987)

[79] M. Berz "Differential Algebraic Description of Beam Dynamics to Very High Orders" Part. Accel. vol. 24, pp. 109-124 (1989)

[80] M. Berz "Arbitrary Order Description of Arbitrary Particle Optical Systems" Nucl. Instr. Meth. vol. A298 pp. 426-440 (1990)

[81] V. Garczynski "On the Differential Algebraic Underlying the COSY INFINITY Computer Code Due to M. Berz" BNL AD/AP-47 (1992)

[82] V. Garczynski “Remarks On Differential Algebraic Approach to Particle Beam Optics M. Berz” Nucl. Instr. Meth. vol. A334 pp. 294-298 (1993)

Map Normal Form:

[83] A.J. Dragt “Nonlinear Lattice Functions” Proceedings of 1984 Summer Study on the Design and Utilization of the Superconducting Super Collider, Snowmass, Colorado, R. Ronaldson and J. Morfin, (eds.) Am. Phys. Soc. (1985)

[84] A. Bazzani, P. Mazzanti, G. Servizi, and G. Turchetti “Normal Forms for Hamiltonian Maps and Nonlinear Effects in a Particle Accelerator” Nuovo Cimento, vol. B 102, pp. 51-80 (1988)

[85] E. Forest, M. Berz, and J. Irwin “Normal Form Methods for Complicated Periodic Systems: a Complete Solution Using Differential Algebra and Lie Operators” Part. Accel. vol. 24, pp. 91-107 (1989)

[86] E. Forest “A Hamiltonian-Free Description of Single Particle Dynamics for Hopelessly Complex Periodic Systems” J. Math. Phys. vol. 31, no 5, pp. 1133-1144 (1990)

Synchrotron Radiation:

[87] M. Sands “The Physics of Electron Storage Rings” SLAC-121 (1970)

[88] K. Hirata and F. Ruggiero “Treatment of Radiation in Electron Storage Rings” CERN LEP Note 611 (1988)

[89] A.W. Chao “Evaluation of Beam Distribution Parameters in an Electron Storage Ring” J. Appl. Phys. vol. 50, No. 2, pp. 595-598 (1979)

[90] K. Ohmi, K. Hirata and K. Oide “From the Beam Envelope Matrix to Synchrotron Radiation Integrals” Phys. Rev. E, vol. 49, no. 1, pp. 751-765 (1994)

Accelerator Modeling and Design:

[91] E. Forest and J. Milutinovic “Leading Order Hard Edge Fringe Fields Effects Exact in $(1+\delta)$ and Consistent with Maxwell’s Equations for Rectilinear Magnets” Nucl. Instr. Meth. vol. A269, pp. 474-482 (1988)

[92] E. Forest and K. Hirata "A Contemporary Guide to Beam Dynamics" KEK Report 92-12 (1992)

[93] E. Forest "The Correct Local Description for Tracking in Rings" Part. Accel. vol. 45, pp. 65-94 (1994)

[94] J. Irwin "The Application of Lie Algebra Techniques to Beam Transport Design" Nucl. Instr. Meth. vol. A298, pp. 460-472 (1990)

[95] J. Irwin "Using Lie Algebraic Maps for the Design and Operation of Colliders" Part. Accel. vol. 54, pp. 107-122 (1996)

[96] K. Oide and H. Koiso "Dynamic Aperture of Electron Storage Rings with Noninterleaved Sextupoles" Phys. Rev. E, vol. 47, no. 3, pp. 2010-2018 (1993)

[97] K. Oide "Optimization of Dynamics Aperture for the KEKB B-Factory" KEK Preprint 96-130

[98] J. van Zeijts J.B.J. van Zeijts and F. Neri "The Arbitrary Order Design Code TLIE" the Gosen High Order Optics Codes Workshop, April 1992